A COMPARISON OF FAULT ZONE FABRICS IN NORTHWESTERN VERMONT

by

Barbara A. Strehle and Rolfe S. Stanley

University of Vermont, Burlington Vermont, 05405

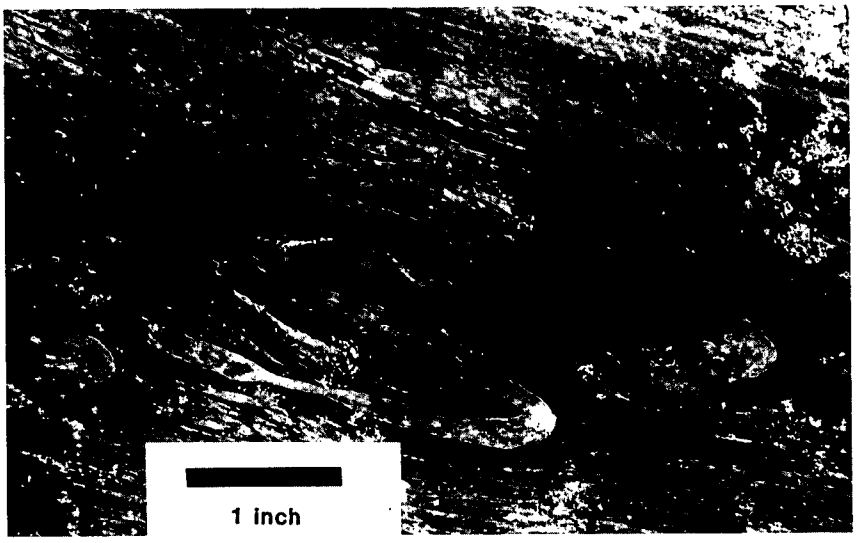

Vermont Geological Survey

Charles A. Ratte, State Geologist

Studies in Vermont Geology No. 3, 1986

TABLE OF CONTENTS

FIGURES

All other figures are shown on Plates 1 - 4.

Cover Picture - F1 folds showing an east-over-west sense of shear in the lower part of the upper plate of the Hinesburg thrust fault, Mechaniscville, Vermont. The S1 schistosity, which is parallel to the axial surface of the F1 folds, is offset by west-dipping shear bands (S 1.5). The view is looking north.

A COMPARISON OF FAULT ZONE FABRICS
IN
NORTHWESTERN VERMONT

by

Barbara A. Strehle and Rolfe S. Stanley
University of Vermont, Burlington, Vermont, 05405

INTRODUCTION

Deformed sedimentary and metamorphic rocks of Precambrian through Ordovician age in western Vermont are dissected by thrust faults of both local and regional scale. Recent mapping by Tauvers (1982), DiPietro (1983 a and b), Karabinos (1984), and Stanley and others (1984,1985) has shown that units formerly considered to be coherent depositional sequences are actually a complex package of thrust slices. The evolution of these faults and associated folds is easier to evaluate in the foreland because much of the evidence used to infer deformational processes is preserved since the rocks are unmetamorphosed and less deformed. In the hinterland, however, much of this evidence is either partially or totally obliterated by syntectonic and posttectonic metamorphism which anneals deformed fabrics and creates new mineral assemblages. The degree to which this evidence is obliterated is a function of the timing of metamorphism and deformation. If ductile faulting occurs during metamorphism, then the resulting fault-zone fabrics consist of well-oriented grains that define a pervasive foliation and a strong mineral lineation. The degree of preferred orientation in the crystal lattices depends on the amount of subsequent recovery and recrystallization. Premetamorphic faults have essentially no unique fabrics because the deformed grains either have been annealed or encorporated into new minerals that are stable under the prevailing temperatures and pressures. These faults are recognized by detailed mapping of lithic units. If the rate of faulting is rapid or if faulting occurs after metamorphism then the fault zone may consist of highly fractured and mineralogically-altered rock that take on many of the characteristics of foreland fault zones. The result of this study illustrates and explains these relationships for northwestern Vermont.

PURPOSE and ORGANIZATION

The purpose of this report is to describe and interpret the fault zone fabrics at four major sites that are located along three thrust faults in the foreland and hinterland of northwestern Vermont. They represent faults zones that developed at progressively deeper levels within the ancient Taconian Mountains.

The fabrics described in this study record the mechanisms of deformation and sense of shear within brittle/ductile fault zones of both the foreland and the hinterland. The structures which are preserved within individual minerals, and the new minerals which grew during the history of the fault zone, provide information on the temperature, pressure, and rate of deformation that prevailed during their formation.

The interpretations presented herein are based on the results of previous observational, experimental and theoretical studies in the fields of rock deformation, material science and structural petrology. One of the major conclusions of this study is that fabrics which record the evolution of the fault zone become progressively obscured by syntectonic and post-tectonic metamorphism. Thus, the Arrowhead Mountain thrust fault in the foreland records a more complete history of deformation than the well-recystallized, simplier fabrics of the Underhill thrust zone in the hinterland. The Hinesburg thrust fault represents physical conditions that are transitional between the foreland and the hinterland.

LOCATION of FIELD AREAS

The four field sites selected for investigation all lie to the east of the trace of the Champlain thrust fault (Fig. 1). The sites form a discontinuous transect from the foreland to the hinterland and, as such, comprise a sequence that crosses north-trending structural and metamorphic zones of northwestern Vermont.

The areas have recently been mapped at scales of 1:12,000 to 1:24,000 (Gillespie, 1975; Tauvers, 1982; Dorsey and others, 1983; and DiPietro, 1983b). The dominant rock types are quartzite, dolostone, metabasite, gneiss, schist, and metagraywacke. The textures vary from cataclasites in the foreland (Arrowhead Mountain thrust fault) where fragmentation by fracturing and grinding overshadows the growth of new minerals in the fault rocks to mylonites in the hinterland (Underhill thrust fault) where recrystallization and recovery in plastically-deformed grains and the growth of new grains and minerals are the dominant processes in the formation of the well-oriented, fine-grained fabric of the fault rocks. The use of the terms "cataclasite" and "mylonite" conforms to the definitions by Sibson (1977). The metamorphic grade varies from sub-chlorite to garnet from west to east. Because a large quantity of experimental data is available on quartz deformation, the structures within quartz in each fault zone are the basis for inferring the mechanisms and physical conditions of deformation.

METHODS of ANALYSIS

At each of the fault localities, structural data on the orientation of slickenlines, mullions, mineral lineations, fold axes, axial surfaces, and foliations were measured with a Brunton compass and recorded on detailed maps and photomosaics. The abundance and change in character of the features at different distances above and below the major slip surface of the thrust fault were also noted. At each locality, except the Underhill thrust fault near Jerusalem, the fault surface is exposed as a clear, well-defined structural and stratigraphic discontinuity. At these locations, oriented samples were collected at specific distances from the fault surface in order to detect strain gradients related to the fault. In Jerusalem, the outcrop is less continuous and the thrust fault is not represented by a single surface but rather it is distributed over a wider zone which is characteristic of faults associated with synmetamorphic faults in the hinterland.

For all the localities the structural features are grouped sequentially into generations or events (i.e, F1, S1, F2, S2) that are based on cross-cutting relations. For example F1 is the earliest recognized folding event to deform bedding or compositional layering. It may have a prominent foliation, S1, parallel to its axial surface. F2 would then represent a younger generation recognized by the fact that it deforms S1. In some localities such as the Hinesburg thrust fault, a very local generation is recognized, which developed between two regional events. Rather than renaming all the regional events, these local events are designated with a decimal point, for example, S 1.5 where the number after the decimal point only means that it occurred sometime between S1 and S2. These generations are therefore a relative time scale to which other structures can be related. Although they are time transgressive across strike, they can commonly be correlated throughout a region (several 7 1/2 minute quadrangles). Errors in correlation, however, may occur in zones of high strain such as fault zones or in traverse across the mountain belt. Despite possible errors of correlation, the fold generations represent events in the progressive deformation associated with the period of mountain building known as the Taconian orogeny appproximately 470 m.y. ago.

For each oriented sample two orthogonal sections were cut perpendicular to the foliation. One section was cut parallel to the lineation and labelled the XZ plane. The X direction parallels the lineation whereas the Z direction is perpendicular to the foliation. The other section was cut perpendicular to the lineation and labelled the YZ plane. Here the Y direction is perpendicular to the lineation and parallel to the foliation. Throughout the text and accompanying plates, the letter X or Z following a sample letter and/or number indicates a section parallel to the lineation (X) or perpendicular to the lineation (Z), respectively. For each of the field areas the penetrative foliations and lineations are an important fabric of the fault zone. These fabric directions can be correlated to the principal planes and axes of the finite strain ellipsoid (Nicolas and Poirier, 1976). The dominant penetrative foliation is considered to be the plane of flattening of the finite strain ellipsoid whereas the prominent mineral lineation represents the direction of maximum finite elongation (Brunel, 1980). The XZ thin section therefore is oriented perpendicular to the plane of flattening and parallel to the direction of maximum elongation.

In thin section the structures within and between minerals were noted and the age relations were determined on the basis of cross-cutting relations outlined by Spry (1969), Vernon (1976, 1977, 1978) and Ferguson and Harte (1975). The prevailing metamorphic conditions within the Hinesburg and Underhill thrust faults were inferred from assemblages of coexisting minerals. The presence of microscopic shear-sense indicators was noted and, upon reorientation of hand samples, the deduced sense of shear was applied to the fault zone and compared to field indicators. Stereographic nets have been prepared for structural field data and crystallographic data. In each of the following sections a description of the outcrop fabrics is followed by a description of thin section fabrics. Representative illustrations and information from each of the fault zones is presented in four plates, each devoted to a single fault locality. The discussion begins in the foreland at Arrowhead Mountain and ends in the hinterland along the Underhill thrust

fault. A complete description and comprehensive discussion of this study appears in Strehle (1985) and is available at the Bailey-Howe Library at the Unversity of Vermont.

ARROWHEAD MOUNTAIN THRUST FAULT

The Arrowhead Mountain thrust fault in Milton, Vermont is located 7 km east of the Champlain thrust fault within a gently deformed and imbricated foreland-cover sequence. Dorsey and others (1983) have interpreted the thrust fault to be located along the sheared, lower limb of the west-verging, overturned Arrowhead Mountain anticline, which plunges gently to the south (Pl. 1, Fig. 1). Arrowhead Mountain is formed by the resistant Cheshire Quartzite of the upper plate and is surrounded by pasture lands underlain by the more erodible Skeels Corner Formation. The east-dipping S1 cleavage in the Skeels Corner Formation flattens as the thrust contact is approached.

Outcrop Fabrics

At the fault exposure, the argillaceous quartzite of the lower member of the Cheshire Quartzite is thrust over the Skeels Corner Formation, a calcareous shale. Slivers of Dunham Dolomite, averaging 50 cm in thickness, occur along the fault surface (Pl. 1, Figs. 1 & 2).

In the slivers of dolostone discontinuous anastomosing stylolitic surfaces, defined by micaeous and carbonaceous material, are locally developed and occur either parallel to or inclined to the dominant S1 foliation observed in the surrounding rocks. Thin (1 cm) fairly continuous, planar surfaces, hereafter referred to as slip surfaces, parallel the fault contact (Pl. 1, Fig. 2). They are light to medium gray in color and have a cherty microcrystalline appearance. One such surface appears to maintain continuity for a minimum horizontal distance of approximately 12 m. In places, a less regular network of slip surfaces is developed; they persist for short distances and terminate against more continuous ones. Slip surfaces trend N11E 18E; slickenlines developed along these surfaces trend S89 E9 (Pl. 1, Fig. 3).

The dolostone is cut by fractures that produce a massive blocky appearance except at the immediate contact with the Cheshire Quartzite and with the Skeels Corners Formation (Pl. 1, Fig. 2). The contact with the quartzite is sharp; it is marked by a foliated, highly fissile zone called the transitional unit which is less than 10 cm thick in the dolostone (Pl. 1, Figs. 4 and 5). Within this zone, the foliation strikes N2W and dips to the east at about 40 degrees. The lower contact with the shale of the Skeels Corners Formation is equally sharp because of the difference in rock composition, although the fault-related strain is harder to document because the shale is incompetent and poorly exposed.

The quartzite consists of interlayered fine- to medium-grained quartz arenite and highly bioturbated fine-grained argillaceous quartzite (Dorsey and others, 1983). At Arrowhead Mountain, the dominant, east-dipping, regional schistosity (S1) forms an anastomosing cleavage defined by black insoluble

residue which ranges from irregular and discontinuous to quasi-planar and pervasive. Where the cleavage is developed it weaves around porphyroclasts of quartz, plagioclase and microcline. Sericite-rich beds are also dominated by anastomosing black films. Based on this characteristics, the S1 cleavage is interpreted to have formed by pressure solution. The black, carbon-rich films represent the insoluble residue whereas the numerous quartz -carbonate veins and quartz or sericite beards on pyrite represent the sinks where the dissolved material from the cleavages was deposited. As the thrust surface is approached this cleavage becomes more closely spaced and is rotated 25 degrees eastward to shallower dips. Within 35 cm of the thrust fault, the quartzite displays a mylonitic texture and is heavily impregnated in places with thin recrystallized quartz veins oriented at diverse angles to S1. This zone represents the transitional unit in the quartzite.

The relative displacement of the Arrowhead Mountain thrust fault was to the west. Evidence for this conclusion is found at a number of places in the fault zone where a closely-spaced cleavage is rotated into near parallelism with either slip surfaces in the dolostone or the contact between the dolostone and the overlying quartzite. This cleavage, called a fault-zone cleavage, developed during early movement on the different slip surfaces because it is spacial restricted to a several centimeter zone on both sides of the surfaces. Subsequent movement has rotated the closely-spaced cleavage into near parallelism with the slip surfaces to produce C-S fabrics. In such places as the dolostone-quartzite contact, the closely-spaced cleavage can be traced into the rotated S1 cleavage. The fault-zone cleavage, however, is younger than S1 because it is more closely spaced than S1 in the overlying quartzite although some of the individual selvedges may have developed from the older rotated S1 surfaces. These relations also suggest that the fault zone cleavage in the dolostone is younger than S1. Small imbricate slices of dolostone along the dolostone-quartzite contact also indicate east-over-west movement.

The rock formations at Arrowhead Mountain are very weakly metamorphosed. Doll and others (1961) show them to be in the chlorite zone of the greenschist facies. Only minor amounts of chlorite are observed in the lower member of the Cheshire Quartzite.

Thin Section Fabrics

Dolostone Fabrics. There is considerable variation in the deformation fabrics displayed by the dolostone, quartzite and shale. The fabrics in the dolostone are generally cataclastic (Pl. 1, Fig. 6). The ratio of matrix to porphyroclasts in the cataclastic material varies among samples. Although one might expect more ground-up matrix and fewer porphyroclasts (a high ratio) as the fault surface is approached, no systematic trend could be identified. The matrix appears dark, turbid, and murky. Such an appearance is due to the very high birefringence of the thoroughly pulverized dolostone and clay. Dolomitic porphyroclasts occur both as single grains and as recemented fragmented grain aggregates or "ghost porphyroclasts" (Pl. 1, Figs. 7 and 8). The ghost porphyroclasts, which are surrounded by the lighter fine-grained matrix, have angular to subrounded outlines. Their appearance is similar to the ghost porphyroclasts identified by Logan and others (1979) in experimental

calcite shear zones. Other porphyroclasts are poorly sorted and are subrounded to angular (Pl. 1, Fig. 6).

The stylolitic surfaces and pressure-solution seams in the dolostone consist of micas and opaque (carbonaceous) material. They are usually discontinuous and commonly define a crude anastomosing foliation (Pl. 1, Figs. 7 and 8). The stylolitic surfaces and pressure-solution seams are widely spaced even where they are well developed. Elongated porphyroclasts are formed where their sides are truncated by pressure-solution selvedges which cut through the cataclasites (Pl.1, Fig. 8).

The slip surfaces consist of ultrafine, 10 to 15 micron diameter quartz grains (Pl. 1, Figs. 7 and 8) which display a strong preferred orientation of c-axes at a high angle to slip surface margins. The strong crystallographic orientation along with the very fine grain size support an origin by dynamic recrystallization (Tullis and Schmid, 1982). The thin layer of quartz, which defines the slip surface, is therefore a mylonite.

In some thin sections pressure-solution cleavages in the dolostone are rotated through an angle of shear of 25 degrees so as to nearly parallel the slip surfaces (Pl. 1, Figs. 7 and 8). This rotation indicates that the slip surfaces are younger than the pressure-solution cleavage and suggests that the deformation mechanism has changed from pressure solution in the cleaved domain to dislocation creep along the slip surface. The sense of shear determined from the rotation of the pressure-solution cleavage is east-over-west.

Quartzite Fabric In thin section the lower member of the Cheshire Quartzite contains mostly quartz with minor amounts of plagioclase and lesser amounts of microcline porphyroclasts. Carbonate is locally abundant. Small (approximately 15 microns) pyrite cubes and pyrite pseudomorphs (hematite) are disseminated in some samples. In thin section the quartzite has an unmodified to slightly recrystallized detrital microstructure. The quartzite is essentially undeformed except for the development of the anastomosing pressure-solution cleavage (S1).

In the thin zone (35 cm) above the fault surface between the dolostone and the quartzite, the quartzite is highly foliated and fissile (Pl. 1, Figs. 2 and 5). A typical rock from this zone contains quartz and plagioclase porphyroclasts (less than 40 microns) surrounded by a dark matrix of very fine sericite, recrystallized quartz (new grains), and carbonaceous material. Quartz porphyroclasts show undulose extinction and deformation lamellae. Some plagioclase grains are fractured whereas other grains show wedge-shaped deformation twins. The foliation is pervasive and defined by black carbonaceous laminations and oriented sericite. The rocks from this zone therefore contain evidence of brittle and ductile processes -- cataclasis, pressure solution, and dislocation creep. It is impossible, however, to determine whether these deformation mechanisms operated simultaneously or were sequentially. The Arrowhead Mountain thrust fault is locally rooted and has moved less than 800 m (Dorsey and others, 1983). It is therefore likely that the fabrics resulted from a complex interplay of and overprinting by competing deformation mechanisms in different minerals and material.

Many of the samples from this zone are cut by several generations of quartz veins varying in thickness from 4 to 80 microns (Pl. 1, Fig.9). Quartz within veins is almost entirely recystallized to very fine, 5 to 25 micron diameter new grain aggregates. Some veins are planar and others are tightly buckled as a result of dissolution in the surrounding rock. The different generations of veins developed during the time when the cleavage formed because they cut and are cross-cut by the cleavage selvedges. These veins, along with other quartz-carbonate veins, sericite beards, and quartz fibers around pyrite grains represent depositional sites for the material dissolved from the pressure-solution cleavage (Pl. 1, Fig. 9).

Summary

In summary, the rock fabrics demonstrate that most of the fault-related deformation is confined to the dolostone slivers and the lowest 35 cm of the Cheshire Quartzite. Although the extent of fault-related deformation in the Skeels Corner Shale can not be assessed because it is poorly exposed, it is assumed to be distributed through a far thicker section than it is in the overlying quartzite. Within the dolostone and quartzite abundant evidence exists for cataclasis, pressure solution, dislocation glide, dislocation creep, and recrystallization. Some of these mechanisms are clearly superimposed such as those described for the dolostone. In the quartzite, however, it is difficult to separate these mechanisms into a sequence, although pressure solution clearly developed before the other mechanisms because it is found outside the highly-deformed transitional unit where the evidence for all these mechanisms occurs.

Interpretation of Fault Zone Mechanics and Evolution

The microscopic features discussed in the preceding section are summarized in Figure 10 (Pl. 1) along with their proposed mode of origin. The manner in which these features are interrelated and their significance to the evolution of the fault zone and the conditions of deformation will be described in the following section.

Fault rocks at Arrowhead Mountain offer convincing evidence for repeated fault motion including changes in deformation mechanisms and the complex superposition of fabrics during the evolution of the fault zone. Much of the evidence is found in the dolostone slivers and in the quartzite near the fault surface. From cross-cutting relations between distinctive microstructures, we can reconstruct the chronology of events shown in Figure 11 (Pl. 1).

The oldest recognizable deformation fabric is the cataclastically deformed dolostone slivers in the fault zone. Based on this evidence we infer that cataclastic flow was one of the first deformation mechanisms to occur along the fault. This would coincide with stable sliding and homogenous behavior in the dolostone that correlates with behavior at relatively shallow levels in the earth's crust. The fault developed when the overturned limb of the fold became progressively attenuated. When the fault was not moving it is likely that the pulverized dolostone was cemented. Renewed movement refractured the dolostone and produced the clasts of breccia within the finer grained matrix.

Subsequent movement along the fault was restricted to a narrow zone now represented by the tectonized transitional quartzite and slip surfaces in the dolostone sliver. We suggest that the deformation mechanism changed from cataclastic flow over a fairly wide but unspecified zone to displacement along continuous surfaces within a fairly narrow zone. Logan and others (1979) documented a similar relationship in experimental fault zones and concluded that the abrupt change in deformation from pervasive cataclastic flow to concentrated slip along fractures was related to energy considerations. With progressive grain size reduction, the energy nessary to continue such processes increases exponentially. In essence, the rock strain hardens. The concentration of slip on discrete surfaces suggests that the fault zone may have produced earthquakes in the past (Sibson, 1977).

At Arrowhead Mountain small dolostone lenses in the fault zone were embedded in the tectonized transitional unit during sliding at the dolostone-quartzite interface. The carbonate-rich nature of the tectonized transitional unit indeed suggests that pulverized dolostone was also encorporated into this unit during deformation. Continued westward movement along the fault bent the closely-spaced S1 foliation in both the overlying quartzite and underlying dolostone slivers.

The decrease in grain size during cataclasis favored a change to a deformation mechanism sensitive to grain size. Pressure solution became the dominant mode of deformation. High fluid pressures may have developed during this time because the dolostone was finely comminuted, indurated, and rich in clay. Such an impervious layer of material can act as a seal or cap to contain fluid under high presssures (Morrow and others, 1984), which would reduce the effective normal stress (Gretener, 1981). Subsequent fracturing would increase permeability and lead to a rapid dissipation of fluid pressures. These events would be followed by a renewed cycle of fluid generation, fracturing, and stress build up. The dense network of veins that impregnate the samples closest to the thrust fault (tectonized transitional quartzite) provide evidence for the occurrence of repeated fracturing and fluid circulation. With increased displacement in the fault zone, Y fractures, which parallel the fault boundaries, develop. Fractures in this orientation have been documented in both natural and experimental fault zones (e.g., Logan and others, 1979). The orientation of the quartz-rich slip surfaces at Arrowhead Mountain strongly suggests that they may be filled Y fractures. The dilatancy associated with fracturing provided the pathways for migration of quartz-rich fluids generated by continuing pressure solution in the quartzite.

The late stages of fault movement are characterized by heterogeneous behavior. Renewed movement is restricted to the quartz-rich slip surfaces, and strain is accommodated by extensive recrystallization.

THE HINESBURG THRUST ZONE

The Hinesburg thrust fault separates the Cambrian-Ordovician rocks of the imbricated carbonate-siliciclastic platform from the older, highly deformed,

metamorphic rocks of the eastern hinterland. Dorsey and others (1983) have shown that the thrust fault occurs along the overturned, sheared limb of a recumbent fold (Pl. 1, Fig. 1). To the south of Mechanicsville, in the Lincoln area, Tauvers (1982) and DiPietro (1983b) have observed that the thrust fault dies out in the overturned limb of the Lincoln anticline. Thus, the Hinesburg thrust fault appears to be similar in style and evolution to the Arrowhead Mountain fold and thrust couple, except that the structure is larger, the displacement is greater, and the deformation is more ductile. Dorsey and others (1983) estimate the displacement to be between 8 and 10 km. in the Hinesburg area.

The Mechanicsville exposure is reached by private unpaved road which intersects a local road leading north from Hinesburg near the Champlain Valley Union High School (Pl. 2, Fig. 12). The exposure is easily seen from the road because quartzite of the hanging wall forms 30 m. vertical cliffs above the gently sloped, less resistant, phyllite and marble of the lower plate.

Outcrop Fabrics

At the Mechanicsville exposure the lower 40 m of the Cheshire Quartzite is structurally overturned along the base of the upper plate of the Hinesburg thrust fault. Higher up the cliff the Cheshire Quartzite grades into the stratigraphically-older Fairfield Pond Formation of Tauvers (1982).

A compositional layering (S0) is defined by alternating layers of sandy quartzite, metasiltstone, and dark phyllite. Sericite and elongate grains of quartz are oriented parallel to S0 and define a foliation that is largely destroyed by the younger foliation within a 10 to 15 m zone above the fault surface where the pervasive foliation, particularly near the fault surface, is really a composite foliation made up of S0 and a younger foliation (S1). Here the foliation has a satiny luster and is mylonitic.

The origin of this compostional layering is a problem. It looks very much like bedding in those parts of the Cheshire Quartzite where the layers of quartzite, metasiltstone, and phyllite vary in thickness. Here the compositional layering is quite different in pattern from the false bedding found in strongly folded and foliated rocks where the layering alternates from one rock type to the other and the thickness of each rock type is about the same. A foliation, however, does parallel S0. This foliation is the dominant feature of the rocks as the Cheshire becomes more phyllitic and grades into the Fairfield Pond Formation in the upper plate. Fold hinges related to the "bedding-plane" foliation have not been observed. We suggest that the "bedding-plane" foliation is related to the Hinesburg recumbent fold of Dorsey and others (1983) and that the associated, west-over-east, parasitic folds on the overturned limb of the major structure fold have been destroyed by fault-related shear.

Within a zone 10 to 15 m above the thrust fault the compositional layering (S0) is deformed into tight isoclinal folds with a pervasive axial surface schistosity, S1 (Pl. 2, Figs. 13 and 15). This schistosity is the result of pressure solution and simple shear. The compositional layering (S0) becomes more severely transposed by S1, which also becomes closely spaced and

pervasive, as the thrust surface at the base of the cliff is approached. Furthermore, F1 folds become more tightly folded and "sheared out" in layers of the same composition. These folds are younger than the Hinesburg recumbent fold because they indicate east-over-west movement rather than west-over-east movement required by the overturned section of Cheshire-Fairfield Pond at Mechanicsville.

S1 strikes N20W and dips 11E (Pl. 2, Fig. 14a). Lineations, which occur on S1 and the composite S0-S1 foliation, trend S75E and plunge at 10 degrees (Pl. 2, Fig 14c). In equal-area projection, F1 fold axes are distributed along a great circle striking N31W and dipping 12E (Pl.2, Fig. 14e). This great circle is essentially parallel to S1. All these folds are asymmetric and indiciate an east-over-west sense of shear. The bisector of the 80 degree separation arc plunges 5 degrees to the S51E. The statistically determined point maxima of fault-related lineations plot within the separation arc and indicate that the Hinesburg slice moved westerly along a line oriented north of west (Pl. 2, Figs 14c & 14d). Within 5 m of the thrust surface the S1 schistosity or the composite foliation is deformed in a few places by a younger, discontinuous, west-dipping foliation, S1.5 (Pl. 2, Fig. 20). This younger foliation is interpreted to be a shear band and, as such, its asymmetry indicates east-over-west displacement. These older fabrics, in turn, are gently deformed by younger F2 folds which possess a poorly developed, east-dipping, axial-surface schistosity, S2 (Pl. 2, Fig. 14b).

Many generations of quartz veins are found throughout the quartzite, particularly in the lower part of the cliff near the thrust surface. The more conspicuous ones are commonly less than 8 cm thick and are oriented either parallel to the compositional layering or S1. Those that are oriented parallel to S1 are very distinctive in that they are milky white, fine grained and laminated. They are found along beds of quartzite where they develop in east-dipping clusters either near the west-facing short limbs of F1 folds or in unfolded segments of the quartzite (Pl. 2, Fig. 13). Although the veins are folded by F1 in a few places, their ends are rotated into the S1 schistosity. This geometry indicates an east-over-west sense of shear (Pl. 2, Figs 16 & 17).

North-trending, vertical fractures dissect the outcrop and are thought to be associated with nearby Mesozoic faults and thus have nothing to do with the thrust-related fabrics (Stanley, 1980). Some of these fractures are filled by quartz or quartz and carbonate. The veins are commonly fibrous and the minerals are not recrystallized. Rare kink folds (F3) are related to the late fractures because their axial planes are parallel to them (Pl. 2, Fig 18).

Along the base of the cliff, slivers of dolostone and calcareous black phyllite are found along the thrust surface
directly below the Cheshire Quartzite (Pl. 2, Fig. 19). The dolostone is light grey on the fresh surface and weathers to a pale buff color. Stylolites are anastomosing and weakly developed. Numerous quartz and quartz-carbonate-plagioclase veins are present. They are sub-perpendicular to the thrust surface.

The black phyllite is very fissile and the pervasive schistosity (S1) is defined by fine-grained aligned white mica and carbonaceous laminae which are either the remains of bedding or an earlier pressure-solution cleavage. Limonitic sandstone lenses and layers are prominent. Pyrite grains are surrounded by well developed pressure fringes of quartz fibers.

Thin Section Fabrics

Samples were collected from the quartzite and dolostone exposed along and above the trace of the Hinesburg thrust fault (Pl. 2, Fig. 19). Texturally, many of the quartzite samples are members of the mylonite series as defined by Sibson (1977), White (1982), and Wise and others (1984). The exact classification, however, is ambiguous for those samples where porphyroclasts are relatively undeformed and quartz segregations are either partially or totally recrystallized. Most of the samples within 0.5 m of the thrust surface are ultramylonites. Many of these samples are phyllonitic because they are rich in mica and have the silky appearance of phyllites.

Quartzite The lower member of the Cheshire Quartzite consists of alternating layers of recrystallized quartz and sericite. The sericite layers contain stilpnomelane, chlorite, and porphyroclasts of quartz, plagioclase and minor microcline. Within a 5 m zone above the thrust surface, pyrite and chlorite are abundant in the sericite-rich layers. Shear bands (S1.5) are also present (Pl. 2, Figs. 20 & 21).

The quartzite within 0.5 m of the thrust surface (Pl. 2, Fig. 19, samples MHT 24, 25, & 26) has a homogeneous and thoroughly mylonitized fabric compared to rocks farther from the fault (Pl. 2, compare Fig. 24 with Figs 22 & 23). Most quartz grains are small and extensively recrystallized. Some quartz occurs as thin (less than 15 microns), very elongate ribbons which are parallel to the pervasive schistosity and consist of aggregates of new grains with aspect ratios up to 75:1 (Pl. 2, Fig. 24). Other quartz grains look like double-tailed comets with a central eye-shaped pod and elongate tails of finer-grained quartz. The quartz in the core and tails is recrystallized. Within the sericite-rich layers, the porphyroclasts become elongate and are aligned parallel or only slightly oblique to the pervasive schistosity. In those samples with the double-tailed comet structure, the quartz-rich layers and porphyroclast-rich layers can no longer be distinguished. Based on the foregoing description, the pervasive schistosity near the fault surface is a mylonitic foliation (Sm). This foliation has developed from the ductile deformation of minerals which define the S1 schistosity and the older layering in the Cheshire Quartzite away from the fault surface. Sm is essentially parallel to S1. The well-defined lineation on Sm is made up of elongate quartz grains, grain clusters, and fibers.

Pyrite porphyroblasts are very numerous in samples near the fault surface (Pl. 2, Figs. 20 and 21). The majority of the grains are late to post S1 (Sm) and pre- to syn-S1.5. Almost all grains exhibit quartz fiber "pressure shadows". The quartz occurs as straight and curved fibers with simple and composite arrangements. The direction of elongation of most of the fibers or composite fiber geometries is discordant to Sm and the shear bands (S1.5). A

few grains have fibers parallel to S1 nearest the pyrite and, overgrowing that, are fibers nearly parallel to S1.5. Pyrite grains closest to the fault surface have the longest fibers. If our interpretation of the S1.5 foliation as shear bands is correct, then the relation between the fiber direction and the shear bands suggests that the rock has undergone some flattening either before or during the formation of the shear bands.

In samples collected 3 m from the fault surface, the quartz grains have modified, smooth boundaries and commonly display undulose extinction or polygonization. The common grain size is much larger than it is in samples within 0.5 m of the fault surface (Pl. 2, compare Fig. 24 with 22 and 23). Many of the grains have deformation lamellae and Boehm lamellae. Although some quartz has short recrystallized tails, quartz ribbons and elongate double-tailed comet grains are absent. The porphyroclasts in the sericite-rich layers vary in diameter from 15 to 350 microns, with the common size falling between 40 and 80 microns. Most grains are equant, although plagioclase commonly occurs in slightly tabular shapes because fractures follow the mineral cleavage (Pl. 2, Fig. 23 and 25). Recrystallization has occurred along the margins of some of the broken pieces. Some of the porphyroclasts are undulose and exhibit curved, bent, and tapered twins which are caused by deformation. Microcline only shows undulatory extinction. In general, the porphyroclasts in the sericite-rich layers are less deformed than the quartz in the extensively-recrystallized, quartz-rich layers.

Quartz porphyroclasts in vein layers are much different from those described from the sericite-rich layers because their size and degree of preservation is variable. All veins are partially to completely recrystallized, with the exception of those associated with the Mesozoic fractures. The shapes of porphyroclasts in vein layers is highly irregular and their boundaries are serrated and embayed due to recrystallization. The porphyroclasts are commonly undulose and in grains with deformation bands, new grains (15 to 55 microns) commonly nucleate at the band boundaries subdividing the host grain into elongate tabular segments (Pl. 2, Fig. 25). New grains also occur along the margin of host grains where they become elongate in mica-rich areas.

Dolostone The dolostone directly below the fault surface is injected with a dense network of veins consisting of comb-fiber and mosaic quartz, plagioclase and carbonate. The veins belong to a number of generations and are oriented at diverse angles to the fault. Veins vary in width from 100 microns to several millimeters. Some of the quartz within the veins is undulose, others have deformation bands, and still others exhibit new grains. The dolostone consists of fine- to very fine-grained inequidimensional, interlocking, anhedral dolomite grains (Pl. 2, Figs. 26 & 27). Stylolites are jagged, anastomosing and discontinuous surface with concentrations of sericite and opaque material. They show no recognizable preferred orientation. The uniformly fine-grain size of dolomite is compatible with an origin by recrystallization whereas stylolites formed by pressure-solution processes.

Summary

In summary, a number of definite trends occur in the upper plate as the fault surface is approached. The samples become more homogeneous, finer-

grained, and the number of porphyroclasts decrease. As a result, the difference between the quartz-rich and sericite-rich layers gradually disappears. The samples therefore grade from protomylonites to ultramylonites. Chlorite and pyrite increase and ribbon quartz becomes more abundant. The quartz in the pressure shadows around pyrite increases in length and porphyroclasts become more elongate and flattened in the dominant schistosity. Many of these features are responsible for the silky, well foliated and lineated appearance of the quartzite.

In sections cut perpendicular to the lineation and foliation, the schistosity (S1/Sm) is more anastomosing and the grains do not appear to be as elongate as they are in sections cut parallel to the foliation. Furthermore, the quartz pressure shadows around pyrite are either absent or shorter and less regularly developed compared to what is seen in sections cut parallel to the lineation. Again these differences become more pronounced as the fault surface is approached.

In the slivers along the fault zone, the dolostone has deformed by recrystallization, pressure solution and fracture. Numerous veins have formed and have been subsequently deformed by ductile processes of dislocation creep and recrystallization. The pervasive schistosity in the phyllite is likely the product of fault movement because it is found directly below the ultramylonite of the upper plate.

Interpretation of Fault Zone Mechanics and Evolution

The fault rocks of the Hinesburg thrust fault are intensely deformed and the strain is distributed over a wider zone than it is at the Arrowhead Mountain thrust fault. Minor structures within the lower member of the Cheshire Quartzite represent an excellent record of the deformation mechanisms and provide a basis for interpreting the evolution of the fault zone. Figure 28 (Pl. 2) summarizes all the deformation features observed in minerals and shows the inferred origin and deformation mechanism for each feature. Evidence for pressure solution, dislocation glide, dislocation creep, and recrystallization is present in all the samples. Ductile rather than cataclastic deformation therefore was the predominant mechanism.

The evolution of the Hinesburg thrust zone at Mechanicsville can be divided into a number of discrete events which are based on cross cutting relations of foliations and folds. The structures and associated deformation mechanisms which occurred during each of these events are listed in Figure 29 (Pl. 2). With the exception of the youngest event (D3) of Mesozoic fractures and kink folds, all the earlier events are considered to be a part of the progressive evolution of the Hinesburg thrust fault, beginning with its inception along the attentuated, and overturned limb of the Hinesburg recumbent fold (D1) during lower greenschist metamorphism and ending with broad folding of the thrust surface during the formation of the Hinesburg synclinorium (D2). Based on the analysis of asymmetric F1 minor folds, slickenlines and microstructural shear-sense indicators, we suggest that the upper plate of the Hinesburg thrust moved westward during D1 time.

The abundant quartz veins are inferred to have developed throughout S1 formation because some of them are parallel to compositional layering (S0) and others are parallel to the S1 foliation. Thin "Z" shaped veinlets which branch from the larger veins and beds of quartzite were subsequently rotated into parallelism with S1 as they are traced from the main vein or quartzite bed to their tails. The discordant segments within the main part of the larger quartzite beds or veins are best interpreted as east-dipping faults (P shears of Logan and others, 1979) and not tension fractures because they are not oriented parallel to the inferred direction of maximum compressive stress which was responsible for westward movement of the thrust.

The exact mechanism by which mylonitic veins such as these develop parallel to faults is unknown. Because they are deformed by F1 folds they must have developed along ductile faults early in D1 deformation. The fact that the veins are now parallel to S1 is best explained by subsequent flattening during which they were rotated into the S1 orientation.

Pressure solution was the dominant deformation mechanism throughout the progressive thinning of the overturned limb of the Hinesburg recumbent fold. This thinning and accompanying shearing eventually formed a discrete sliding surface that is presently located along the quartzite-dolostone contact in the Mechanicsville area. Sometime during this event, the S1 foliation became mylonitized so that the quartzite near the thrust surface became very fine grained, intensely foliated (Sm) and strongly lineated. Recrystallization of the dolomite and extensive flowage in the phyllite most likely correlate with mylonitization of the quartzite. The abundance of quartz and chlorite in the quartzite and quartz-carbonate veins in the dolostone near the fault surfaces suggests that fluids permeated the fault zone during or shortly after this time. It is possible that the reduction in grain size by recrystallization near the fault surface, which would increase the grain-boundary porosity by virtue of an increase in grain-boundary area, might promote diffusion of fluids that migrated along the foliation near the fault surface. A process such as this has been described by White and Wilson (1978).

During D1.5, renewed westward movement along the fault rotated S1 and the older quartz veins to produce the "Z" shaped quartz digitations. Dislocation creep and pressure solution were the dominant deformation mechanisms during this time. The majority of pyrite growth is associated with this event because individual grains are euhedral and cut across the mylonitic schistosity (Sm). The densest concentrations of pyrite occur in a zone from the fault up approximately 2 m. The shear band foliation (S1.5) is restricted to the mylonites and ultramylonites near the fault and is best developed in mica-rich rocks. Only one shear-band orientation is found, which suggests that this structure resulted from simple shear rather than flattening (White, 1979). The direction of shear is east-over-west.

Pressure solution continues to be important through D1.5. Well-developed quartz fiber pressure shadows grow oblique to Sm and, in samples displaying the shear band foliation, the trend of fiber elongation in some of the grains parallels S1.5. The fact that pressure shadows are best developed and have the highest fiber elongation ratio in XZ sections (northwest-southeast), whereas they are short and rare in YZ sections (northeast-southwest), is

evidence that almost no extension has occurred parallel to Y, the strike direction. This conclusion agrees with the inferred direction of movement from the shear-band geometry.

D2 (F2) caused folding of the thrust fault. Broad undulations are apparent along the thrust surface. Minor F2 folds are locally developed throughout the quartzite. They are open folds and are not associated with pervasive cleavage formation. Localized recrystallization (dislocation creep) is also associated with D2 because post-Sm veins are recrystallized.

D3 is not related to fault emplacement. It is associated with Mesozoic normal faulting (St. George Fault) and brittle fracture (Stanley, 1980). Numerous vertical fractures dissect the outcrop. Rare kink folds, with axial planes parallel to the fractures, are also present although rare (Pl. 2, Fig. 18).

Although extensive recrystallization has occurred in quartz-rich layers, sufficient evidence has been preserved so as to reconstruct the history of deformation before and during chlorite-grade metamorphism. As will be seen in the following sections, deeper-seated thrust faults, evolving in the hinterland to the east, have undergone pervasive ductile flow. Any evidence of events which may have occurred prior to mylonitization during higher grade syntectonic metamorphism in these rocks has been erased. The Hinesburg thrust fault therefore represents an intermediate or transitional zone between the Arrowhead Mountain and the Underhill thrust zones.

THE UNDERHILL THRUST FAULT

The Underhill thrust zone consists of a number ductile thrust faults that, along with the Hinesburg thrust fault, mark the boundary between imbricated shelf sequence and a complex package of thrust slices in the higher grade pre-Silurian eugeoclinal rocks to the east (Fig. 1; Stanley and Ratcliffe, 1983, 1985). The faults of the Underhill thrust zone are commonly marked by slivers of greenstone, quartzite and or Middle Proterozoic gneiss. These relations are well displayed in two localities, in the hills directly north of Jerusalem and the bridge at South Lincoln (Pl. 3 and 4). These two localities were studied in detail so as to understand how fault-zone fabrics are preserved in metamorphic rocks of different mechanical properties. The Underhill thrust zone is located along the eastern margin of the Lincoln massif where DelloRusso (1986) has mapped a number of separate thrust faults. Stanley and Ratcliffe (1983, 1985) suggest that the Underhill thrust zone correlates with the Hoosac Summit thrust fault and Middlefield thrust zone along the eastern border of the Middle Proterozoic Berkshire Massif in western Massachusetts (Zen and others, 1983).

SOUTH LINCOLN LOCALITY

Tauvers (1982) and DelloRusso (1986) have identified several slivers of mylonitic Middle Proterozoic plagioclase gneiss of the Mt. Holly Complex along the faults of the Underhill thrust zone. One of these slivers is well exposed at the bridge at South Lincoln along the east bank of the New Haven River where the outcrop extends for a distance of approximately 17 m (Pl. 3, Figs. 30, 31, and 32). Here the sliver contains plagioclase gneiss and the overlying basal conglomerate of the Late Proterozoic Hoosac Formation. The Grenville unconformity is preserved in the sliver. The rocks of the footwall are biotite schist that occur stratigraphically higher in the Hoosac Formation.

Outcrop Fabrics

The mylonitized granitic gneiss displays a well developed, penetrative foliation (Sm) defined by grain elongation of quartz and plagioclase and the alignment of subhedral micas. The foliation in the gneiss west of the bridge strikes N14E and dips 60 east (Pl. 3, Fig. 33a). A well developed mineral lineation on Sm plunges to the southeast (Pl. 3, Fig. 33b). Younger crenulations related to F2 folds, which fold the South Lincoln sliver, are sporadically developed and best displayed in highly micaceous samples of the gneiss.

The schist below the thrust fault is divided into two units based on a change in composition and appearance from the dark gray, biotite schist to a green, calcareous chlorite schist. Large biotite grains randomly cut the dominant foliation in the biotite schist. The dominant foliation in the schist is the regional S1 schistosity although minor F2 folds also deform the thrust fault and the S1 schistosity (Pl. 3, Fig. 30).

Thin Section Fabrics

Mylonitic Gneiss. Although samples of the Mt. Holly Complex in the sliver were collected at distances progressively farther from the South Lincoln thrust contact (Pl 3, Fig. 31) no variations in strain where detected. The fabrics are very homogeneous in all samples. The mylonitic foliation is defined by elongate grains of quartz and plagioclase and tabular grains of biotite, muscovite, and chlorite. This foliation is planar in sections cut parallel to the lineation, but it becomes anastomosing in sections cut perpendicular to the foliation (Pl. 3, Figs. 35 and 36).

Both plagioclase and quartz within the granitic gneiss have undergone extensive recrystallization. New grains make up 60 to 80% of a given sample. They range in size from 40 to 200 microns with an average of 80 microns. New grains of plagioclase are slightly elongated (~3:1) whereas new grains of quartz are more commonly polygonal. New grains of both minerals have smooth and curving boundaries. The new grains of plagioclase and quartz nearest the margins of the older host grains are commonly equant and polygonal. New grains of plagioclase have simple and polysynthetic twins. Quartz grains are usually slightly undulose with larger grains displaying banded extinction or

faint deformation bands. These characteristics indicate that the new grains have been deformed during recrystallization.

The shape and appearance of grains and the foliation are a function of the orientation of the thin sections relative to the mineral lineation. In sections cut perpendicular to the lineation (YZ sections) the grain shape is equant and polygonal. Many grains develop a foam texture (soap-bubble network) characteristic of annealed grains. The foliation also has an anastomosing geometry. In sections cut parallel to the lineation (XZ sections) the new grains are elongate and the foliation is planar. The end sections of short rods that define the mineral lineation in outcrop are revealed therefore in the YZ plane.

Porphyroclast of quartz in the matrix and those that occur in layers ("elongate domains") paralleling the foliation are very different. Quartz porphyroclasts within the matrix range in size from 200 to 600 microns in diameter. They are irregularly shaped and have slightly embayed scalloped margins. These grains are undulose and commonly have deformation bands.

The elongate domains are one to several grains in width and form continuous bands parallel to Sm (Pl. 3, Fig. 37). Quartz grains within the domains are subrectangular in shape with aspect ratios of 5:1. Most of the grains are undulose and display either banded extinction or sharp deformation bands. Some grains are segmented into large (150 microns) subgrains. The deformation bands are subperpendicular to the direction of grain elongation and to the foliation; the bands parallel the c-axis. White (1976) has stated that elongate grains with the c-axis direction perpendicular to the foliation plane and with deformation bands perpendicular to the direction of grain elongation, indicate slip along the basal plane (0001) of quartz.

Quartz c-axis analysis of sample SL3, which has well developed elongate domains, yielded a diffuse pattern with multiple maxima (Pl. 3, Fig. 38). The sample population consisted almost entirely of grains belonging to elongate domains. Quartz grains within these bands have sub-rectangular shapes. They are coarse-grained and have smooth, curving boundaries. Most grains have deformation bands parallel to the trace of the c-axis. Dislocation climb, which resulted in the formation of deformation bands during recovery, would not be expected to contribute to a preferred crystallographic orientation. If anything, it would be expected to weaken pre-existing fabrics unless slip were occurring at the same time. Dislocation climb therefore is thought to be the agent responsible for the diffuse c-axis pattern.

Plagioclase porphyroclasts occurring in the matrix either appear blotchy or have undulose or irregular extinction. Their boundaries are irregular and scalloped. New grains are common along the margins of the porphyroclasts. The porphyroclasts are heavily clogged with inclusions of mica and other very fine-grained (less than 8 microns) optically unidentifiable particles. Although these inclusions are probably caused by retrograde metamorphism of the Middle Proterozoic gneiss, they may be related to deformation.

Muscovite and biotite occur as blades and elongate shreds defining the foliation. Some grains are slightly undulose where a grain is bent. These grains are oriented parallel to the mylonitic foliation and their mildly deformed nature provided evidence that they are syn- to post-Sm phases.

Fine needle-like flakes of muscovite are also found dispersed within the matrix. They are oriented oblique to Sm. These grains are interpreted to be the recrystallized remnants of older grains with relict pre-Sm orientation. Stubby parallelogram-shaped muscovite and biotite grains are rare and occur only in micaeous layers. Their terminations are slightly toothed (i.e., they are not rational crystal faces). Their shape is considered to be a result of solution rather than crystallographic slip based on the nature of their terminations and shape (Mancktelow, 1979). Larger subhedral grains occurring oblique to Sm are late-Sm phases. They provide evidence that metamorphism outlasted the deformation event or rather, that highest temperatures were achieved in the late stages of emplacement.

The mylonitic foliation (Sm) is folded tightly in some layers (Pl. 3, Fig. 39). The folds are especially apparent in mica-rich samples. A later crenulation cleavage is developed sporadically and is related to F2 folds because they fold the thrust surface and are very different in style from the tight folds just described. Biotite grains oriented at random angles to the mylonitic foliation are present in some samples (Pl. 3, Fig. 41). They post-date the formation of the crenulation cleavage and provide information that the F2 event occurred at least at biotite-grade conditions.

The foliation, which is defined by elongate domains, new grains, and oriented mica in the YZ sections, appears much different in the XZ sections where the foliation assumes an anastomosing geometry. This fabric results from the foliation wrapping around the globular end sections of grains which are elongated in the X-direction (Pl. 3, Fig. 42).

Hoosac Formation. Sample SL13 (Pl. 3, Fig. 31), a phyllonite, was collected from the lower part of the basal conglomerate of the Hoosac Formation just above the unconformity with the Mount Holly gneiss. It is radically different, in composition and appearance, from other samples of the gneiss. It is very rich in muscovite, chlorite and biotite, and also contains abundant anhedral magnetite grains, some of which are replaced by chlorite. Muscovite occurs as dense mats which enclose elongate porphyroclasts and new grains of quartz and plagioclase. Biotite occurs as large blades which are commonly oblique to Sm. Quartz also occurs in layers which parallel Sm. A weak crenulation related to F2 overprints Sm.

Sample SL12 (Pl. 3, Fig. 31) collected from the Hoosac Formation underlying the gneiss, is similar to SL13. SL12, however, contains very coarse poikolitic biotite prophyroblasts and albite porphyroblasts. Biotite grains are oblique to Sm. The S2 overprint is stronger and appears more as kink bands rather than gentle crenulations. Sample SL11 (Pl. 3, Fig. 31), collected from the Hoosac Formation closest to the thrust contact with the gneiss, consists of quartz and plagioclase porphyroclasts and new grains in a matrix of disoriented chlorite and epidote. The preferred orientation of mica and the phyllonitic textures displayed by other schist samples are absent. This

fabric must have developed after fault emplacement when chlorite developed with the influx of fluids during late to post-fault movement.

Interpetation of Fault Zone Mechanics and Evolution

The mylonitic rock of the Middle Proterozoic Mt. Holly complex is very homogeneous in terms of deformation features and fabric. The only variation between samples is in the percentage of mica. Sm is the dominant foliation, although the dispersed fine mica flakes oblique to Sm suggest an earlier foliation. Crenulations are sporadically developed and post-date Sm. The down-dip lineation defined by quartz rods is pervasive and maintains a consistent orientation. Tight folds of Sm are also present in some samples. They are related to folding of the mylonitic foliation during renewed movement that occurred before the late S_{ϵ} crenulation.

The dominant mechanism of deformation in the mylonitic gneiss has been dislocation creep (Pl. 3, Fig. 43). The unit is almost entirely recrystallized. Both plagioclase and quartz have undergone recrystallization. Quartz in elongate domains exhibits evidence of recovery. Only a small number of irregularly shaped and generally elongate plagioclase porphyroclasts remain in the matrix; this is significant in that it indicates that temperatures obtained were greater than 450° C (Voll, 1976). Quartz is not observed as porphyroclasts except in elongate domains. New grains are much coarser than those in quartz-rich layers of the Hinesburg thrust fault samples, which is consistent with their higher temperature origin (Etheridge and Wilkie, 1981).

The South Lincoln rocks display a distinct layering of quartz and feldspar. The elongate domains of quartz are similar to what Bouchez (1982) and Bouchez and Pecher (1981) describe as ribbon microstructure. Bouchez (1982) suggested that quartz was segregated during deformation by diffusion and that feldspar remained in the layers between the quartz ribbons. Bouchez and Pecher (1981) conclude that the prismatic subboundaries (deformation bands) resulted from low temperature stress imposed after the main deformation responsible for the ribbons. Subsequent grain growth occurred at elevated temperatures. Such an origin is compatible with observations of the South Lincoln samples.

Because deformation has occurred at temperatures where recrystallization has been so pervasive, most of the early history has been obliterated. The chronology of events relating to fault evolution therefore is more speculative at South Lincoln compared to the Arrowhead Mountain and Mechanicsville fault zones. The sequence of events inferred from microstructural evidence is in accord with experimental, theoretical, and field investigations on ductile shear zones (Pl.3, Fig. 44).

The Middle Proterozoic rocks were first metamorphosed during the Grenville orogeny, 1.0 to 1.1 billion years ago. These rocks are similar in composition to other gneisses in the Lincoln massif (DelloRusso, 1986), although thorough Paleozoic mylonitization has obliterated any textural resemblance to less deformed samples. Fine, recrystallized mica oblique to Sm may be the only remnant of an earlier foliation.

Initial Paleozoic deformation occurred under upper greenschist to epidote-amplibolite facies conditions where the temperature was greater than 450°C since plagioclase has undergone extensive recrystallization. Epidote was produced during breakdown of plagioclase. Some plagioclase grains became highly elongated and persisted as porphyroclasts. The recrystallized plagioclase occurred as small new grains which accommodated considerable strain. After initial grain-size reduction, the anisotropy, which was introduced by recrystallization and grain elongation, provided pathways for diffusion. Such grain-size sensitive processes as diffusion creep were favored. The strain rate began to decline. Temperatures persisted at a high enough value to allow nucleation of muscovite and biotite which grew parallel to Sm. Quartz also segregated into elongate domains parallel to Sm during this event. Deformation bands in the elongate domains of quartz reflect the occurrence of a late stress pulse that may be related to renewed movement along the fault.

Metamorphism outlasted the deformation event because biotite and muscovite occur as subhedral, stubby grains that grew at random angles to Sm in mica-rich layers. The late F2 folds and crenulations which deform the thrust zone at South Lincoln probably developed before this growth event. Similar mineral and fold relations are found in the Late Proterozoic-Lower Cambrian schists to the east and west of this locality (DelloRusso, 1986; O'Loughlin, 1986; Lapp, 1986). It is likely that exsolution (?) features in the plagioclase of the gneiss can be correlated to this event and subsequent cooling.

JERUSALEM LOCALITY

Further north near Jerusalem, the Underhill thrust fault is exposed over a much wider zone. In this locality the fault zone is delineated by tectonic slivers of metabasite and quartzite which occur along its trace (Pl. 3, Fig. 45). Samples were collected from the fault zone and the adjacent upper plate of the Underhill slice. The following were considered: 1) quartz sericite schist and metagreywacke (CZU), 2) biotite-rich metagreywacke and greenstone, and 3) greenstone (CZUg).

Outcrop and Thin Section Fabrics

Much of the fault rock consists of quartz mylonites. The quartz-rich samples were useful in evaluating the deformation behavior and response of quartz and comparing the results to the quartz-rich rocks of other fault zones in western Vermont. In addition, quartz c-axis fabrics were determined from these samples. The mineralogy in the metabasite provided information on the conditions of metamorphism.

The mylonitic foliation, Sm, is pervasive within the fault zone (Pl. 4, Fig. 46). The down-dip mineral lineation developed on Sm surfaces is strong and undeflected in the area.

The samples most useful for universal stage analysis were those that contained primarily quartz. Sample 3D is a quartz mylonite with only minor amounts of dispersed sericite flakes and thin mica laminae; it is almost

entirely recrystallized (Pl. 4, Fig. 47). The contoured projection of 253 quartz c-axes resembles an asymmetric type I crossed girdle (Pl.4, Fig. 48a; Lister, 1977). The pattern, however, is diffuse. The fabric skeleton, obtained by connecting the loci of points of maximum density, shows a clear asymmetry and indicates an east-over-west shear sense. The quartz in mylonite sample 5A exhibits a microstructure involving pronounced grain growth (Pl. 4, Fig. 50). The size of quartz grains in sample 5A is between 60 and 110 microns whereas the grain sizes of quartz in sample 3D range from 25 to 55 microns. The contoured pattern obtained from 180 quartz c-axes in sample 5A is ill-defined but resembles a type I crossed girdle (Pl. 4,Fig. 51). The inferred sense of asymmetry is east-over-west. In both samples 3D and 5D, the pattern of quartz c-axes is diffuse and not sharp like many published samples from quartzites suggesting that it has been distorted by younger deformation.

Evidence for younger deformation is found in many of the fault rocks at Jerusalem. Younger folds and an associated cleavage (F2, S2 of Tauvers, 1982 and DiPietro, 1983) deform the fault zone and developed under at least biotite-grade conditions. Flattening likely occurred perpendicular to S2 because conjugate sets of shear bands, which are oriented symmetrical about S2, were found in the metabasite (samples 2A). In summary, the distinct asymmetry in the quartz fabric skeletons in samples 3D and 5A indicates an early deformation involving simple shear. The sharpness of this pattern was then disrupted by later folding and flattening during pure shear.

The metabasite samples also contained useful shear-sense indicators because they are composed of different minerals of varying grain size. Figure 49 (Pl. 4) shows an asymmetric lense-shaped biotite which indicates an east-over-west displacement sense. Such features as asymmetric overgrowths (sample 2D) and asymmetric pressure shadows (sample 4A) also yielded an east-over-west shear sense.

Although the metabasite samples provide insight into the conditions and history of metamorphism in the area, they proved to be the least informative in understanding the evolution of deformation because little experimental work has been done on mafic rocks or polymineralic rocks in general (Tullis and others, 1982). Thus there is little experimental results with which to interpret our petrographic studies.

The degree of deformation, however, is reflected in the degree of alignment of elongate minerals (epidote, amphibole), and the extent to which micas have been deformed into parallelism. The amphiboles in the metabasite consist of brown hornblende cores with zoned actinolitic rims and discrete grains of patchy zoned actinolite. The hornblende-actinolite grains have quartz and chlorite pressure shadows. Quartz and plagioclase are found in layers and elongate pods. Both minerals occur as polygonal, relatively undeformed grains. Rarely are primary plagioclase grains observed.

Extensive recrystallization has occurred in units other than the metabasites and young undeformed veins. Dislocation creep has been the dominant deformation mechanism. In the spangly- mica schist, however, some original detrital grains of quartz and plagioclase are preserved, generally in the chlorite-rich samples.

SUMMARY OF THE UNDERHILL THRUST FAULT

South Lincoln and Jerusalem samples exhibit evidence that temperatures during the late stages of deformation were sufficiently high to allow for the segregation of quartz and the coarsening of grains. In addition, micas oriented at random angles to the mylonitic foliation at South Lincoln also indicate that post-tectonic temperatures associated with biotite metamorphism were moderate. For both areas we propose that the metamorphic event outlasts the deformation event. Although substantial flattening and biotite-grade metamorphism have altered the fault zone, asymmetrical fabrics are still preserved, particularly at Jerusalem, that indicate simple east-over-west shear. This observation is consistent with current models of faults which predict the development of a metamorphic peak after thrust faulting in the hinterland (England and Richardson, 1977; Holland and Richardson 1979).

The history recorded in metabasite amphiboles along the Underhill thrust fault is less certain at this time. Laird and Albee (1981) have tentatively assigned relative ages to cores and rims in zoned grains. For instance, in one sample (location 29; Laird and others, 1984) the actinolitic rims surrounding barroisite cores could be due to decreasing pressure during uplift or to a second metamorphism. Isotopic-age studies and further amphibole analyses will clarify these problems in the near future.

TECTONIC IMPLICATIONS

Summary of Deformation Trends

Various deformation mechanisms dominate in each of the fault zones described in this study (Fig. 2). In a given fault zone, each rock has responded differently to the imposed strain. For instance, at Arrowhead Mountain, the dolostone has undergone cataclastic flow whereas pressure solution has been the predominant deformation mechanism in the quartzite. These data along with the mineral assemblages have been used to evaluate the pressure and temperature conditions of fault evolution. This information also provides insight to the variation in deformational fabric, intensity, and style across the orogen.

All of the fault-zone features and their controlling variables such as temperature, effective confining pressure, and strain rate are interdependent to some degree. For instance, pressure solution has been shown to dominate at temperatures below 400° C whereas dislocation creep dominates at higher temperatures (Allison and others, 1978). Cataclasis, however, is dependent on effective confining pressure rather than temperature. It is also favored by rapid strain rates in contrast to ductile flow which is more likely to form under slow strain rates.

Mineral composition and grain size will also control the dominant deformation mechanism. Switches in deformation mechanism may occur in response to changes in grain size or pressure-temperature changes. As a result a single

deformation mechanism need not dominate throughout a deformation event. This relations was demonstrated at the Arrowhead Mountain and Hinesburg thrust faults.

Metamorphism may overshadow the effects of deformation where it is associated with post-thrust fault deformation or where the rate of recovery exceeds the rate of strain (Wise and others, 1984). This first condition is illustrated by the South Lincoln locality. This second condition may occur where minerals are consumed faster in metamorphic reactions than they develop strain-free minerals by dislocation flow (Etheridge and others, 1983). The metabasite slivers along the Underhill thrust in Jerusalem illustrates this situation. With the appropriate rock composition, such zoned or partially altered minerals as amphibole and garnet make excellent geothermometers and geobarometers for future work.

The initiating instability leading to the development of fault zones varies according to the location within the orogenic belt. In the foreland, bedding in the layered sequences provide planes of weakness that become faults. Fold-fault couples such as Arrowhead Mountain are found at the ends or tip of the major faults (Boyer and Elliot, 1982). Ramps develop when the thrust fault encounters units of greater competency and steps up section . Fault propagation over ramps produces complex folds and fault stacks (Boyer and Elliot, 1982). In the transitional zone, faults are initiated along weak surfaces related to folds. Overturned limbs of tight or isoclinal folds are attenuated and develop into fault zones such as the Hinesburg thrust fault. In the hinterland, metamorphism may contribute to the formation of reaction softened zones where deformation becomes localized. Softening is a requirement in such homogeneous isotropic rocks as gneisses that make up much of the crystalline basement. It is commonly observed that such softened zones develop along the sheared limbs of isoclinal folds. Fault zones, however, can be localized at lithic contacts either where a strong ductility contrast still persists or where fluids are abundant during metamorphic reactions (Etheridge and others 1983, Fig. 7).

Fluid Participation In Fault Zones

In each of the fault zones, there is evidence that fluids were present during deformation. For example, at the Arrowhead Mountain thrust fault, we suggest that circulating fluids indurated the cataclastically-deformed dolostone so that it became strong enough to support differential stress during the next episode of deformation. Similar events have been postulated for other foreland fault zones (e.g., Brock and Engelder, 1977; House and Gray, 1982). Quartz-rich fluid also migrated into slip surfaces during the late stages of deformation. Numerous layer parallel quartz segregations occur in the quartzite of the upper plate of the Hinesburg thrust fault at Mechanicsville. Slickenfibers occurring on Sl-Sm surfaces and quartz pressure shadows around pyrite also attest to the presence of fluids within the fault zone (Sibson, 1980). The silica was likely generated by pressure solution during cleavage formation. Pyrite and chlorite are also abundant in the vicinity of the Hinesburg thrust fault. In the mylonitic gneiss at South Lincoln, quartz was segregated into elongate domains which are parallel to the mylonitic foliation. Quartz veins are very abundant in the Underhill fault zone further

north in the Jerusalem area (DiPietro, 1983b). These veins range from thoroughly mylonitized to relatively undeformed so that fluid circulation must have occurred during and after deformation.

The presence of fluids along thrust faults has long been recognized as a potential explanation for the paradox of major thrust faults, (Hubbert and Rubey, 1959). The occurrence of numerous calcite and calcite-quartz veins along foreland faults is primary evidence for this relationship. Furthermore, hydrothermal veins, ore deposits, and quartz veins are commonly observed adjacent to faults in other domains. Crack seal microstructures provide further evidence of cyclic fracturing, fluid circulation, and resealing during deformation (Ramsay, 1980). As permeability increases within a fault zone, water is circulated into the zone and subsequently it can reduce frictional resistance if abnormal fluid pressures are developed. High fluid pressures may be maintained by the occurrence of a low permeability layer along the fault surface (e.g., gouge or adjacent to the fault surface (eg.g., crystalline rocks in the hanging wall). An increase in fracturing during faulting may occur and produce the veins that are abundant along mapped faults. At greater depths, these fluids may produce extensive metasomatism along the shear zone rocks (Beach, 1976). Granitic melts may also be localized along deep seated faults. Figure 4 summarizes these observations.

The presence of a fluid will induce other mechanical effects less obvious than hydrofracturing. A fluid may promote reaction softening in which ductility is greatly enhanced by the occurrence of mineral reactions catalyze by the fluid. Such processes may provide sufficient weakening of the rock to permit localization of the shear zone and the attainment of high strain values within a restricted zone. Etheridge and others (1983) have pointed out that the fluid may contribute to changes in the mineral assemblage which may strongly influence the dislocation creep rheology of the rock. These changes are expected to be most pronounced in polymineralic rocks where complex and possibly cyclic mineral reactions occur.

Fault Zone Model

Figure 5 depicts a fault zone model which accounts for the distribution of fault rocks in relation to metamorphic facies, fluid circulation regime, structural regime and deformation regime. Although one major fault zone is shown in the model, it depicts what might be expected along a fault at a specific crustal level. For example, mylonites are expected at deeper levels whereas cataclasites occur at shallower levels. With successive dip slip movement of hanging wall rocks on a thrust fault, mylonites formed at lower depths may be overprinted by more brittle features. According to the evidence presented in this study, each of the faults investigated in northwestern Vermont has been located on the diagram. The pressure and temperature locations have been estimated from diagnostic mineral assemblages and deformation features. The location of the Underhill thrust fault is constrained by pressure and temperature data on amphiboles obtained by Laird and others (1984).

Age of Thrust Faulting

Effects of both Taconian (Ordovician) and Acadian (Devonian) metamorphism are recognized in Vermont. Delineating the exact extent of these effects has proved controversial. Taconian metamorphism is documented west of the Green Mountain massif (GMM) (Harper, 1968; Cady, 1969;Lanphere and Albee, 1974; Laird and others, 1982, 1984; Lanphere and others, 1983). Sutter and others (1985) recognized three distinct domains: 1) a high pressure-low temperature event of T-1 age; 2) a low gradient Barrovian metamorphic event of T-2 age; and 3) a high gradient Barrovian metamorphic event of T-3 age. Isotopic ages for localities in Vermont have been based on K-Ar and 40Ar/39Ar systematics of whole rock and mineral separate samples employing both total fusion and incremental heating techniques. The main Taconian event (T-2) occurred between 460 and 470 million years ago based on these analyses. The T-1 domain is a relict of blueschist-eclogite facies metamorphism associated with subduction whereas T-2 and T-3 correlate to imbrication and loading of eugeoclinal cover rocks and basement slices (Stanley and Ratcliffe, 1985). The maximum grade attained is kyanite-staurolite along the crests of the Precambrian massifs and chlorite to garnet grade elsewhere. In contrast, the Acadian event, established to be 360 to 380 m.y. old, involved retrograde metamorphism of pre-Silurian zones in central and northern Vermont, biotite to sillimanite grade metamorphism of the Silurian and Devonian rocks, and was associated with magmatic activity and widespread dynamothermal effects.

Sutter and others (1985) suggest that the Acadian overprint is limited to areas east of the GMM. They acknowledge, however, that data from the Taconic allochthons in western Massachusetts may reflect an Acadian overprint. They interpret ages obtained from samples west of the GMM which are near the study area to be cooling ages. These age are considered to be a minimum age of Taconian metamorphism that reflect a significant time interval occurring between metamorphism and cooling to the argon closure temperature. Lanphere and others (1983) and Laird and others (1984) find that their data support the existence of Acadian metamorphism west of the GMM. Amphiboles from two samples (at locations both east and west of the Gmm) gave Ordovician ages whereas micas from nearby pelitic schists gave younger ages which they interpret to be the result of Acadian metamorphism. Current isotopic research is designed to resolve the problem.

ACKNOWLEDGEMENTS

This study was made possible by support from the following organizations: U.S. Department of Energy Grant DE-FG02-81WM-46642 awarded to the Vermont Geological Survey, U.S. Forest Service Grant USDA 40-1681-30537 (Green Mountain National Forest) awarded to Stanley, University of Vermont Institutional Grant #2-15886 to Stanley, University of Vermont Mini-Grant award to Strehle. Preparation and publication of this report was supported in part by the National Science Foundation Grant EAR 8516879 (Stanley). Any opinions, finding, conclusions, or recommendations expressed herein are those of the authors and do not necessarily reflect the views of the Department of Energy. Special thanks go to Robbin M. Button, Charles A. Ratte, Murray Journeay, and Brewster Baldwin for their critical review of the manuscript.

REFERENCES

Allison, I., Kerrich, R., and Starkey, J., 1978, The variation of quartz orientation patterns in regional metamorphic tectonites: Neues Jahrbuch fur Mineralogie Abhandlungen, v. 134, p. 92-103.

Armstrong, R.L., and Dick, H.J.B., 1974, A model for the development of thin overthrust sheets of crystalline rock: Geology, v. 2, p. 35-40.

Beach, A., 1976, The interrelations of fluid transport, deformation, geochemistry and heat flow in early Proterozoic shear zones in the Lewisian complex: Philosophical Transactions Royal Society of London, v. A280, p. 569-604.

Bouchez, J. L., 1982, Quartz microstructures associated with the Himalayan Main Central thrust, in Borradaile, G.J., and others, eds., Atlas of deformational and metamorphic rock fabrics: New York, Springer-Verlag, p. 350-351.

Bouchez, J. L. and Pecher, A., 1981, The Himalayan Main Central Thrust Pile and its quartz-rich tectonites in central Nepal: Tectonophysics, v. 78, p. 23-50.

Boyer, S. E. and Elliot, David, 1982, Thrust systems: American Association of Petroleum Geologists Bulletin, v. 66, p. 1196-1230.

Brock, W.G., and Engelder, T., 1977, Deformation associated with the movement of the Muddy Mountain overthrust in the Buffington Window, southeastern Nevada: Geological Society of America Bulletin, v. 88, p. 1667-1677.

Brunel, M., 1980, Quartz fabrics in shear zone mylonites: evidence for a major imprint due to late strain increments: Tectonophysics, v. 64, p. T33-T44.

Cady, W.M., 1969, Regional tectonic synthesis of northwestern New England and adjacent Quebec: Geological Society of America Memoir 120, 181 pp.

DelloRusso, Vincent, 1986, Geology of the eastern part of the Lincoln massif, Central Vermont: [M. S. thesis]: Burlington Vermont, University of Vermont, 255p.

DiPietro, J.A., 1983a, Geology of the Starksboro area, Vermont: Vermont Geological Survey Special Bulletin, no. 4, 14 p.

_____, 1983b, Contact relations in the Late Precambrian Pinnacle and Underhill Formations, Starksboro, Vermont [M.S. thesis]: Burlington, Vermont, University of Vermont, 132 pp.

Doll, C.G., Cady, W.M., Thompson, J.B.,Jr., and Billings, M.P., 1961, Centennial Geologic Map of Vermont: Montpelier, Vermont, Vermont Geological Survey, scale 1:250,000.

Dorsey, R. L., Agnew, P. C., Carter, C. M., Rosencrantz, E. J., and Stanley, R.S., 1983, Bedrock geology of the Milton quadrangle, northwestern Vermont: Vermont Geological Survey, Special Bulletin, no. 3, 14 p.

England, P.C., and Richardson, S.W., 1977, The influence of erosion upon the mineral facies of rocks from different metamorphic environments: Journal Geological Society of London, v. 134, p. 201-213.

Etheridge, M.A., Wall, V.J., and Vernon, R.H., 1983, The role of the fluid phase during regional metamorphism and deformation: Journal of Metamorphic Geology, v. 1, p. 205-226.

_____, and Wilkie, J.C., 1981, An assessment of dynamically recrystallized grain size as a paleopiezometer in quartz-bearing mylonite zones: Tectonophysics, v. 78, p. 475-508.

Ferguson, C.C., and Harte, B., 1975, Textural patterns at porphyroblast margins and their use in determining the time relations of deformation and crystallization: Geological Magazine, v. 112, p. 467-480.

Gillespie, R.P., 1975, Structure and stratigraphy along the Hinesburg thrust [M.S. thesis]: Burlington, Vermont, University of Vermont, 63 p.

Gretener, P.E., 1972, Thoughts on overthrust faulting in a layered sequence: Bulletin of Canadian Petroleum Geology, v. 20, p. 583-607.

_____, 1981, Pore pressure, discontinuities, isostasy and overthrust, in McClay, K.R., and Price, N.J., eds., Thrust and nappe tectonics: Geological Society of London, Special Publication, no. 69, p. 33-39.

Guha, J., Archambault, G., and Leroy, J., 1983, Correlation between the evolution of mineralizing fluids and the geomechanical development of a shear zone as illustrated by the Henderson 2 Mine, Quebec: Economic Geology, v. 78, p. 1605-1618.

Harper, C.T., 1968, Isotopic ages from the Appalachians and their tectonic significance: Canadian Journal Earth Science, v. 5, p. 49-59.

Holland, T.J.B., and Richardson, S.W., 1979, Amphibole zonation in metabasites as a guide to the evolution of metamorphic conditions: Contributions to Mineralogy and Petrology, v. 70, p. 143-148.

House, W.M., and Gray, D.R., 1982, Cataclasites along the Saltville thrust, U.S.A. and their implications for thrust sheet emplacement: Journal of Structural Geology, v. 4, p. 257-269.

Hubbert, M.K., and Rubey, W.W., 1959, I. Role of fluid pressure in the mechanics of overthrust faulting: Geological Society of America Bulletin, v. 70, p. 115-166.

Karabinos, Paul, 1984, Deformation and metamorphism on the east side of the Green Mountain massif in southern Vermont: Geological Society of America, v. 95, p. 584-593.

Lachenbruch, A.H., 1980, Frictional heating, fluid pressure, and the resistance to fault motion: Journal of Geophysical Research, v. 85, p. 6097-6112.

Laird, J., and Albee, A.L., 1981, Pressure, temperature and time indicators in mafic schist: their application to reconstructing the polymetamorphic history of Vermont: American Journal of Science, v. 287, p. 127-175.

_____, Lanphere, M.A., and Albee, A.L., 1984, Distribution of Ordovician and Devonian metamorphism in mafic and pelitic schists from northern Vermont: American Journal of Science, v. 284, p. 376-413.

Lapp, E. T., 1986, Geology of the Mount Grant - South Lincoln area, Central Vermont: [M. S.]: Burlington, Vermont, University of Vermont, 114p.

Lanphere, M.A., and Albee, A.L., 1974, $^{40}Ar/^{39}Ar$ age measurements in the Worcester Mountains: evidence of Ordovician and Devonian metamorphic events in northern Vermont: American Journal Science, v. 274, p. 545-555.

_____, Laird, J., and Albee, M.A., 1983, Interpretation of $^{40}Ar/^{39}Ar$ ages of polymetamorphic mafic and pelitic schist in northern Vermont: Geological Society of America, Abstracts with Progams., v. 15, p. 147.

Lister, G.S., 1977, Discussion: crossed girdle c-axis fabrics in quartzites plastically deformed by plane strain and progressive simple shear: Tectonophysics, v. 39, p. 51-54.

Logan, J.M., Friedman, M., Higgs, N., Dengo, C., and Shimamoto, T., 1979, Experimental studies of simulated gouge and their application to studies of natural fault zones, in Speed, R.C., and Sharp, R.V., organizers, Proceedings of Conference VIII-Analysis of actual fault zones in bedrock, U.S.G.S. Open File Services Section, 70-1239, p. 305-343.

Mancktelow, N.S., 1979, The development of slaty cleavage, Fleurieu Peninsula, South Australia: Tectonophysics, v. 58, p. 1-20.

Morrow, C.A., Shi, L.Q., and Byerlee, J.D., 1984, Permeability of fault gouge under confining pressure and shear stress: Journal Geophysical Research, v. 89, p. 3193-3200.

Namson, J.S., 1982, Studies of the structure, stratigraphic record or plate interaction and role of pore-fluid pressure in the active fold and thrust belt of Taiwan and a study of manganese deposits from northern California [Ph.D. thesis]: Princeton, New Jersey, Princeton University, 379 p.

Nicolas, A., and Poirier, J.P., 1976, Crystalline plasticity and solid state flow in metamorphic rocks: New York, John Wiley and Sons, 444 p.

O'Loughlin, S. B., 1986, Bedrock geology of the Mt. Abraham-Lincoln Gap area, Central Vermont: [M.S. thesis]: Burlington, Vermont, University of Vermont, 164p.

Ramsay, J. G., 1980, Shear zone geometry: a review: Journal of Structural Geology, v. 2, p. 83-99.

Sibson, R.H., 1977, Fault rocks and fault mechanisms: Journal of the Geological Society London, v. 133, p. 191-213.

_____, 1980, Power dissipation and stress levels on faults in the upper crust: Journal Geophysical Research, v. 85, p. 6239-6247.

_____, 1983, Continental fault structure and the shallow earthquake source: Journal of the Geological Society London, v. 140, p. 741-767.

Spry, A., 1969, Metamorphic textures: Oxford, Pergamon Press, 350 p.

Stanley, R.S., 1980, Mesozoic faults and their environmental significance in western Vermont: Vermont Geology, v. 1, p. 22-32.

Stanley, R. S. and Ratcliffe, N. M., 1983, Simplified lithotectonic synthesis of pre-Silurian rocks in western New England: Vermont Geological Survey Special Bulletin, no. 5, 9 p., 2 plates.

----------, 1985, Tectonic synthesis of the Taconian orogeny in western New England: Geological Society of America, v. 96, p. 1227-1250.

Straw, W.T., and Schmidt, C.J., 1981, Heart Mountain detachment fault: a phreatomagmatic-hydraulic hypothesis: Geological Society America, Abstracts with Programs., v. 13, p. 227.

Strehle, B. A., 1985, Deformation mechanisms and structural evolution of fault zone fabrics in northern Vermont: A comparative study: [M. S. thesis]: Burlington, Vermont, University of Vermont, 323p.

Sutter, J.F., Ratcliffe, N.R., and Mukasa, S.B., 1985, Metamorphic and tectonic history of western New England based on $^{40}Ar/^{39}Ar$ and K-Ar data: Geological Society of America, v. 96, p. 123-136.

Tauvers, P.R., 1982, Basement-cover relationships in the Lincoln area, Vermont [M.S. thesis]: Burlington, Vermont, University of Vermont, 176p.

Taylor, S., 1983, The genetic implications of pressure shadows in mylonites of the Hinesburg thrust zone, Mechanicsville, Vermont [unpublished Senior research thesis]: Burlington, Vermont, University of Vermont, 27 pp.

Tullis, J. A. and Schmid, S.M., 1982, General remarks on flow and deformation mechanisms: Structural Geology and Tectonics Division of the Geological Society of America (unpubl. shortcourse notes), 28 pp.

_____, Snoke, A., and Todd, V., 1982, Significance and petrogenesis of mylonitic rocks: Geology, v. 10, p. 227-230.

Vernon, R.H., 1976, Metamorphic processes: New York, John Wiley and Sons, 247 p.

_____, 1977, Relationships between microstructures and metamorphic assemblages: Tectonophysics, v. 39, p. 439-452.

_____, 1978, Porphyroblast-matrix microstructural relationships in deformed metamorphic rocks: Geologische Rundschau, v. 67, p. 288-305.

Voll, G., 1976, Recrystallization of quartz, biotite and feldspars from Erstfeld to the Leventina Nappe, Swiss Alps, and its geological significance: Schweiz. Mineral. Petrogr. Mitt., v. 56, p. 641-647.

White, J.C., and White, S.H., 1981, On the structure of grain boundaries in tectonites: Tectonophysics, v. 78, p. 613-628.

White, S. H., 1976, The effects of strain on the microstructures, fabrics, and deformation mechanisms in quartzites: Philosophical Transactions of the Royal Society London, v. A283, p. 69-86.

_____, 1979, Grain and subgrain size variations across a mylonite zone: Contributions to Mineralogy and Petrology, v. 70, p. 193-202.

_____, 1982, Fault rocks of the Moine Thrust Zone: a guide to their nomenclature: Textures and Microstructures, v. 4, p. 211-221.

_____, and Wilson, C.J.L., 1978, Microstructure of some quartz pressure fringes: Neues Jahrbuch fur Geologie und Palaontologie Abhandlungen, v. 134, p. 33-51.

Wise, D.U., Dunn, D.E., Engelder, J.T., Geiser, P.A., Hatcher, R.D., Kish, S.A., Odom, A.L., and Schamel, S., 1984, Fault-related rocks: suggestions for terminology: Geology, v. 12, p. 391-394.

Zen, E-an, ed., Goldsmith, Richard, Ratcliffe, N. M., Robinson, Peter, and Stanley, R. S., compilers, 1983, Bedrock geologic map of Massachusetts: U. S. Geological Survey and the Commonwealth of Massachusetts, Department of Public Works, and Sinnot, J. A., State Geologist, scale 1:250,000.

All Master of Science theses published by the University of Vermont are available at Bailey-Howe Library, University of Vermont, Burlington, Vermont, 05405.

Figure 1. Interpretative Tectonic Map of Vermont and eastern New York showing the general location of the Arrowhead Mountain thrust fault (AMTF), the Hinesburg thrust fault at Mechanicsville (HTFM), and the Underhill thrust fault at Jerusalem (UTFJ), and South Lincoln (UTFSL). The geological map is taken from Stanley and Ratcliffe (1985, Pl. 1, figure 2a). Symbol T in A6 is a glaucophane locality at Tilliston Peak. Short line with x's (Worcester Mountains) and line with rhombs (Mount Grant) in C6 and D5 mark the Ordovician kyanite-chloritoid zones of Albee (1968). Widely-spaced diagonal lines in northcentral Vermont outline the region that contains medium-high pressure amphibolites described by Laird and Albee (1981b). Irregular black marks are ultramafic bodies. Open teeth of thrust fault symbols mark speculative thrust zones. The following symbols are generally listed from west to east. Yad, Middle Proterozoic of the Adirondack massif; Yg, Middle Proterozoic of the Green Mountain massif; YL, Middle Proterozoic of the Lincoln massif; Y, Middle Proterozoic between the Green Mountain massif and the Taconic slices, Vermont; OCp, Cambrian and Ordovician rocks of the carbonate-siliciclastic platform; rift-clastic sequence of the Pinnacle (CZp) and Fairfield Pond Formations (CZf) and their equivalents on the east side of the Lincoln and Green Mountain massifs, PhT, Philipsburg thrust; HSpT, Highgate Springs thrust; PT, Pinnacle thrust; OT, Orwell thrust, UT, Underhill thrust ; HT, Hinesburg thrust; U, ultramafic rocks; CZu, Underhill Formation; CZuj, Jay Peak Member of Underhill Formation; OCr, Rowe Schist; Om, Moretown Formation; Oh, Hawley Formation and its equivalents in Vermont; JS, Jerusalem slice; US, Underhill slice; HNS, Hazens Notch slice; MVFZ, Missisquoi Valley fault zone; PHS, Pinney Hollow slice; BMT, Belvidere Mountain thrust; CHT, Coburn Hill thrust; Oa, Ascot-Weedon sequence in grid location 7A. Specific locations of each fault zone is shown on larger-scale maps on Plates 1-4.

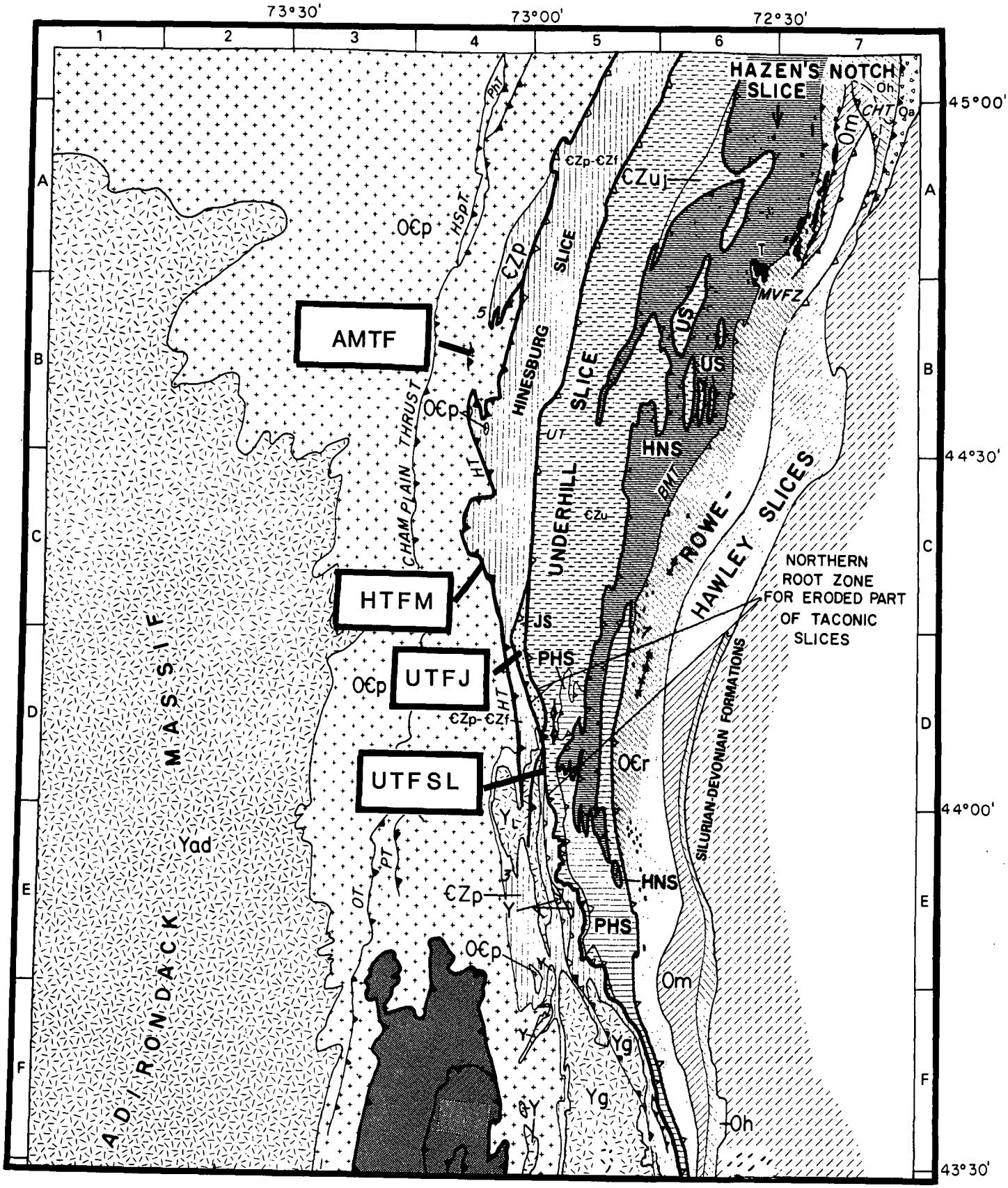
73°30'
73°00'
72°30'
45°00'
44°30'
44°00'
43°30'
HAZEN'S NOTCH SLICE
AMTF
HTFM
UTFJ
UTFSL
CHAMPLAIN THRUST
HINESBURG SLICE
UNDERHILL SLICE
ROWE - HAWLEY SLICES
NORTHERN ROOT ZONE FOR ERODED PART OF TACONIC SLICES
SILURIAN-DEVONIAN FORMATIONS
ADIRONDACK MASSIF
MVFZ
HSpT
PhT
HT
UT
BMT
PT
OT
CZuj
CZu
HNS
PHS
JS
US
Om
Oh
CHT
Qa
Oεr
Yad
Yg
Y
Oεp
CZp
CZp-CZf

Locality	Deformation Mechanism	Rock type and/or fabric domain and/or mineral	Evidence
Arrowhead Mountain thrust fault	Cataclastic flow	dolomite	*poorly sorted angular clasts and grain fragments in a pastelike matrix *fractures *transgranular cracks
	Pressure Solution	dolomite	*stylolites *veins
		quartzite	*veins *solution selvedges *fibrous quartz pressure shadows on pyrite
	Dislocation creep	quartz slip surfaces	*uniformly ultrafine grained quartz with a strong preferred orientation
	Mechanical twinning	dolomite	*twin lamellae
Hinesburg thrust fault	Mechanical twinning & Dislocation glide	plagioclase, microcline and quartz	*mechanical twins (plagioclase) *undulatory extinction
	Dislocation creep	quartzite closest to fault quartz veins	*preferred orientation *subgrains & new grains
	Pressure Solution	quartzite	*solution selvedges *abundant vein quartz *quartz fiber pressure shadows
		dolomite	*stylolites *veins
Underhill thrust fault, South Lincoln	Dislocation creep	plagioclase and quartz	*preferred orientation *undulose extinction *banded extinction *deformation bands *serrated grain boundaries *new grains
Underhill thrust fault, Jerusalem	Dislocation creep	sheared quartz veins, metagraywacke, quartzite, schist	*as above

Figure 2. Synopsis of the operative deformation mechanisms and microstructural evidence for each fault zone.

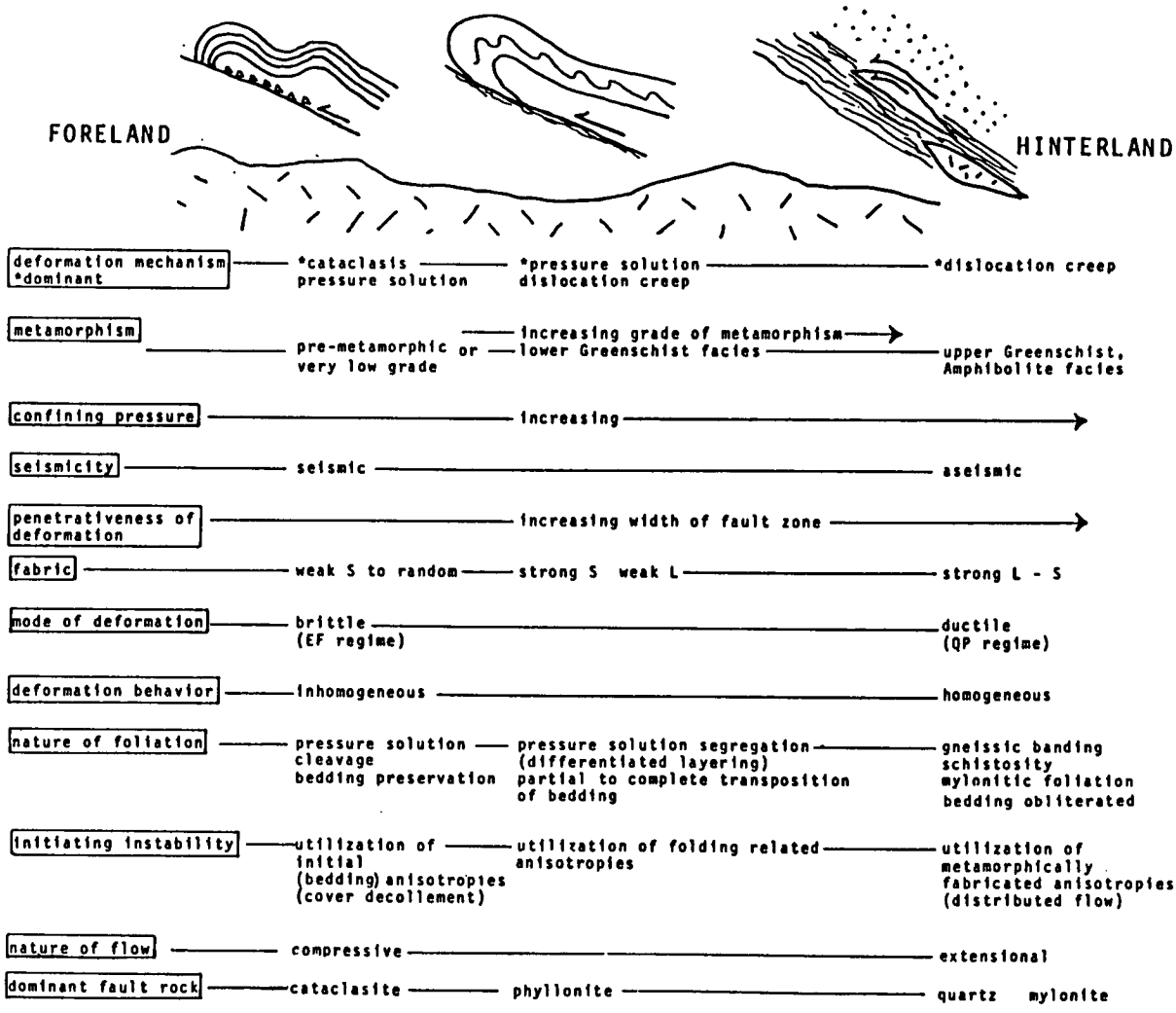

Figure 3. Summary of fault characteristics as revealed in the present-day transect from the foreland, which represents a shallow level in the crust, to the hinterland, which represents a deeper level in the crust.

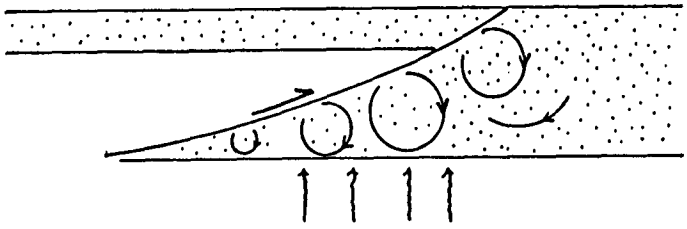

Advective (infiltrative) fluid migration pattern after Etheridge & others (1983)

Mechanisms for attaining high fluid pressure

1. thermal expansion of fluid
   a. shear heating (Sibson, 1973, 1980)
   b. emplacement of hot crystalline sheets (Armstrong & Dick, 1974)
   c. aquathermal pressuring (Namson, 1982)
2. disequilibrium compaction (Gretener, 1972; Namson, 1982)
3. acoustic fluidization (Lachenbruch, 1980)
4. "entrapment" or ponding by seal which acts as an obstacle to further flow

Pathways of fluid migration

1. channeled
   a. hydrofractures
   b. second order faults & fractures
2. grain boundaries (White & White, 1981)
3. dilatant areas created by moving over asperities along the fault surface (Guha and others, 1983)
4. microcracking (Etheridge and others, 1983)

Fluid derived by:

1. dehydration
   a. footwall rocks
   b. clays and other hydrous phases along the slip surface
2. pressure solution
3. compaction
4. phreatomagmatism (Straw & Schmidt, 1981)
5. frictional melting (localized)
6. partial melting

Maintenance of high fluid pressure

An impervious or low permeability layer acts as a seal or cap

1. clay rich gouge
2. shale
3. evaporite
4. crystalline rock

Role of fluid

1. Chemical
   a. enhance diffusion rate
   b. solute and transporting medium
   c. reactant in metamorphic reactions
2. Mechanical
   a. promote microfracturing
   b. reaction softening
   c. reduction in effective normal stress
   d. changes in mineral assemblages influence dislocation creep rheology

Figure 4. Fluid participation in fault zones.

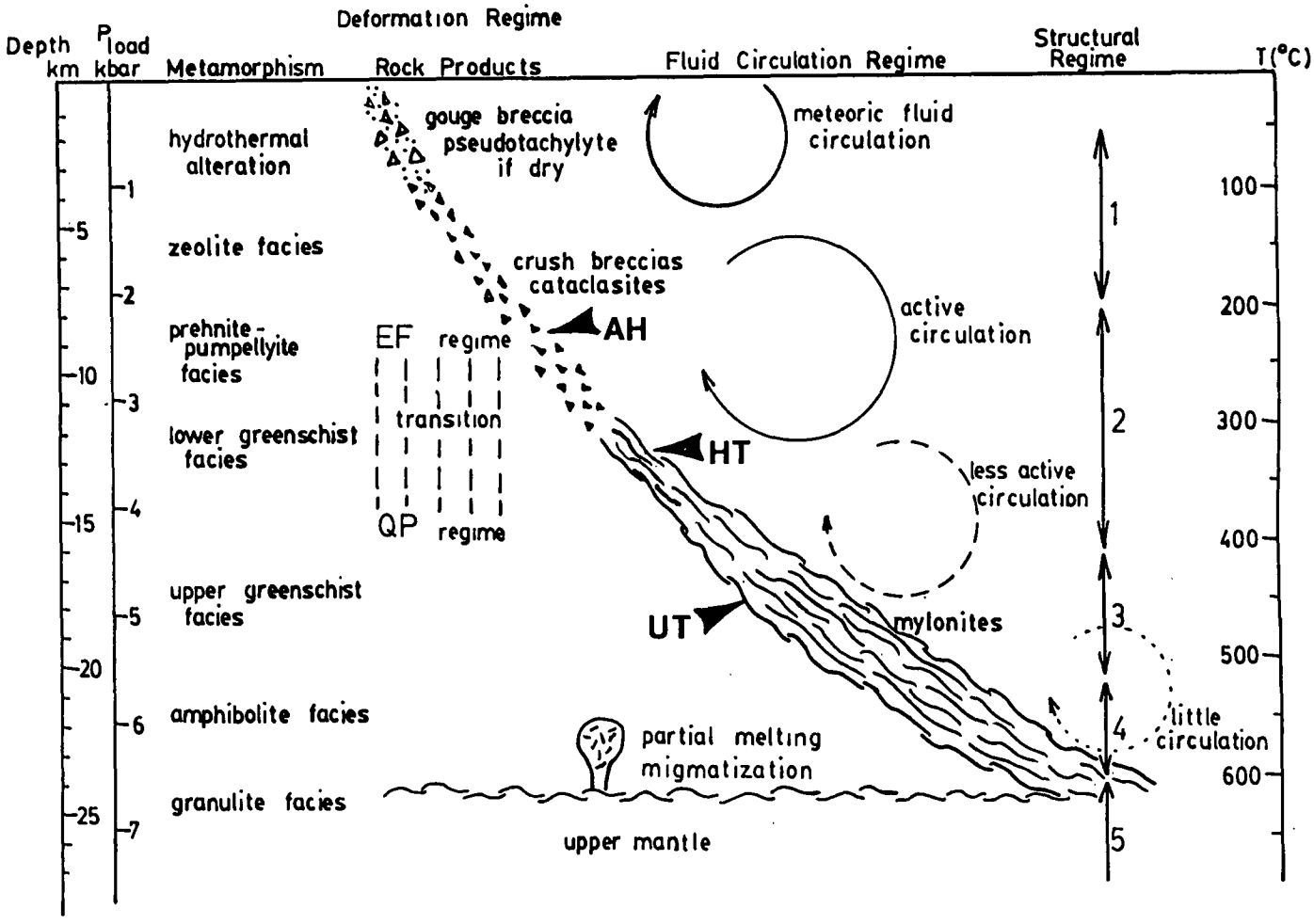

Figure 5. Conceptual model of a major fault zone. Depth (kilometers), pressure (kilobars), and temperature (0C) are indicated. Metamorphic facies, deformation regime, rock products, fluid circulation regime, and structural regime are labelled. The behavior in the first structural regime is strongly influenced by fluid pressure. The second regime involves increased creep rate and similar and recumbent isoclinal folds on all scales. The third regime has a restricted mineralogy and similar rheologies for all the common rock types. The fourth regime involves the formation of gneissic structures and extensive flow folds. The fifth regime is characterized by prolonged laminar flow and simple structural styles. Locations are as follows: AH, Arrowhead Mountain thrust fault; HT, Hinesburg thrust fault; UT, Underhill thrust fault. The location of these faults on the diagram is based on deformation features and mineral assemblages. The location of the Underhill thrust fault is supported by analyses of amphiboles from the Underhill Formation in nearby areas (Laird and Albee, 1981). Pressure solution processes become significant at 250 degrees C and continue to dominate until 400 degrees C where dislocation creep processes take over. Feldspar recrystallization occurs at temperatures that are equal to or slightly above 450 degrees C (Voll, 1976). The diagram is modified from Holland and Lambert (1969), Sibson (1977, 1983), and Etheridge and others (1983).

The Arrowhead Mountain Thrust Fault

Plate 1

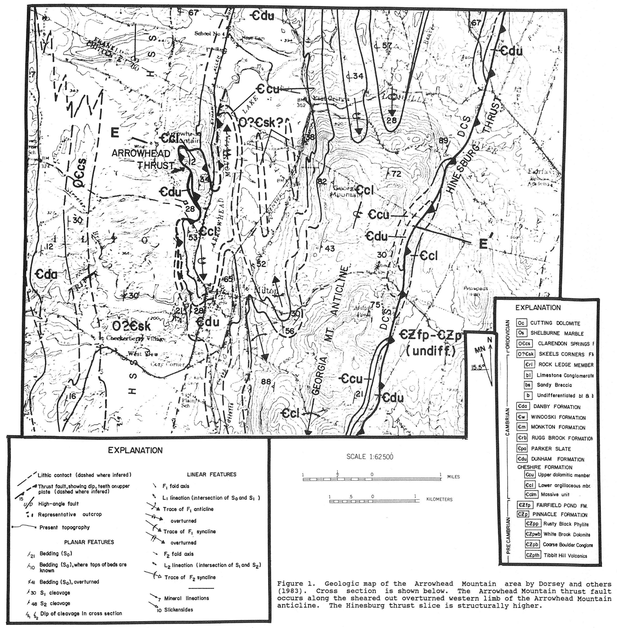

EXPLANATION

- Lithic contact (dashed where inferred)
- Thrust fault, showing dip, teeth on upper plate (dashed where inferred)
- High-angle fault
- Representative outcrop
- Present topography

PLANAR FEATURES

- Bedding (S_0)
- Bedding (S_0), where tops of beds are known
- Bedding (S_0), overturned
- S_1 cleavage
- S_2 cleavage
- Dip of cleavage in cross section

LINEAR FEATURES

- F_1 fold axis
- L_1 lineation (intersection of S_0 and S_1)
- Trace of F_1 anticline
- overturned
- Trace of F_1 syncline
- overturned
- F_2 fold axis
- L_2 lineation (intersection of S_1 and S_2)
- Trace of F_2 syncline
- Mineral lineations
- Slickenlides

SCALE 1:62500

MILES

KILOMETERS

EXPLANATION

	Cls	CUTTING DOLOMITE
	Cs	SHELBURNE MARBLE
	COcs	CLARENDON SPRINGS F
	O?Csk	SKEELS CORNERS FM
	Ccl	ROCK LEDGE MEMBER
	Cl	Limestone Conglomerate
	Cbr	Sandy Breccia
	C	Undifferentiated Cl & C
CAMBRIAN	Cdd	DANBY FORMATION
	Cw	WINOOSKI FORMATION
	Cm	MONKTON FORMATION
	Crb	RUGG BROOK FORMATION
	Cpa	PARKER SLATE
	Cdu	DUNHAM FORMATION
		CHESHIRE FORMATION
	Cbu	Upper dolomitic member
	Ccl	Lower argillaceous mbr.
	Cclm	Massive unit
	CZfp	FAIRFIELD POND FM
	CZp	PINNACLE FORMATION
	CZpq	Rusty Block Phyllite
	CZwd	White Brook Dolomite
	CZcn	Cowee Boulder Conglom
PRE-CAMBRIAN	CZbh	Tibbit Hill Volcanics

Figure 1. Geologic map of the Arrowhead Mountain area by Dorsey and others (1983). Cross section is shown below. The Arrowhead Mountain thrust fault occurs along the sheared out overturned western limb of the Arrowhead Mountain anticline. The Hinesburg thrust slice is structurally higher.

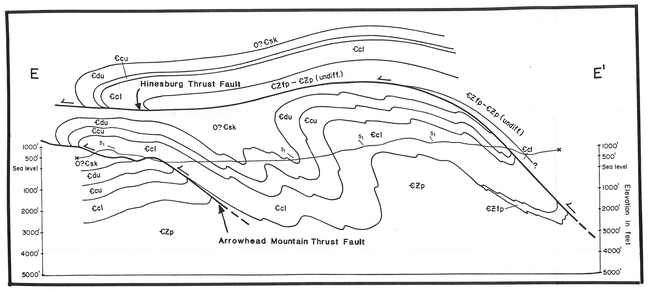

Figure 2. The outcrop sketch shown to the right was prepared from a photomosaic of the fault exposure. It shows the arrangement of stratigraphic units and structural elements for 3 different segments of the outcrop. Sample location sites are also shown. The viewer is looking to the east for the two diagrams labelled "N - S". The viewer is looking to the north for the diagram labelled "W - E". The zone labelled "FOL" is the highly foliated, tectonized transitional unit at the base of the lower member of the Cheshire Quartzite (Ccl). The average attitude of the foliation in this unit is N2E, 40E. Slip surfaces are labelled "SS".

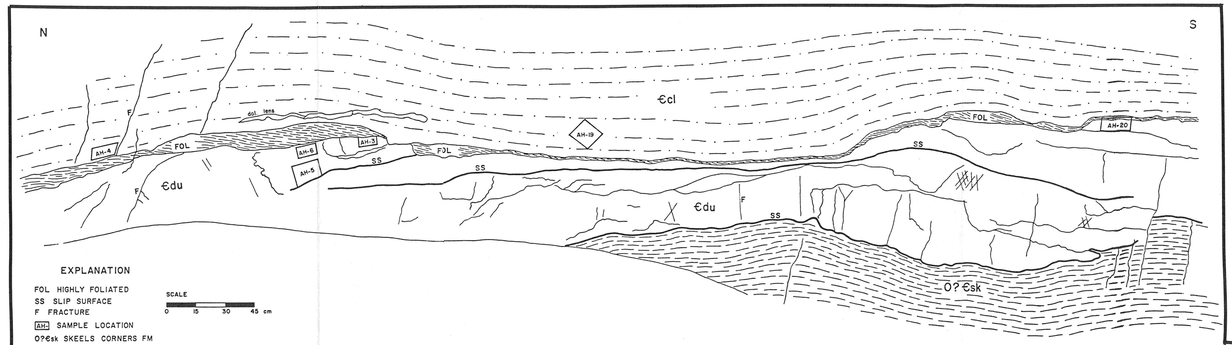

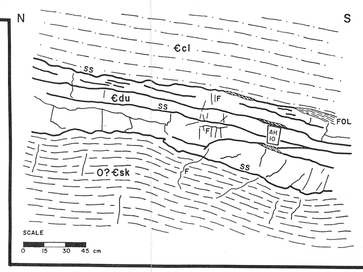

Figure 3. Lower hemisphere equal area projections give the attitude of slickenlines and of slip surfaces which occur within the dolomite. The plane of projection is horizontal with the tick marking the north direction. Contours are given as the percentage of points per 1% area. Slip surfaces are thin, laterally continuous layers which are oriented parallel to the thrust fault boundaries. They have a "cherty," microcrystalline appearance and consist of very fine-grained recrystallized quartz.

Slickenlines

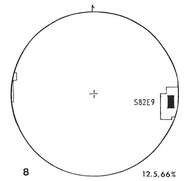

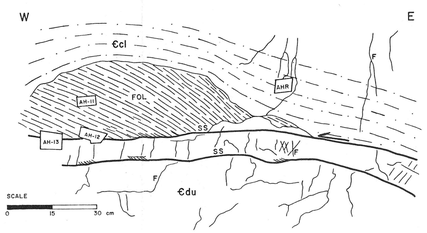

Slip Surfaces

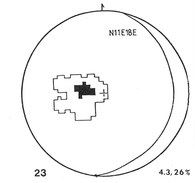

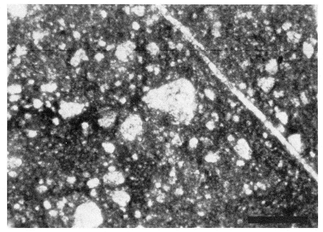

Figure 6. Sample AH 13 is a dolostone cataclastite. It consists of poorly - sorted, angular grain fragments and grain clusters within a turbid, pulverized, and structureless matrix. Later fractures and quartz infillings are planar and cross cut the cataclastic fabric. YZ section. The view is to the east. Cross nicols photograph. Bar scale is 500 microns.

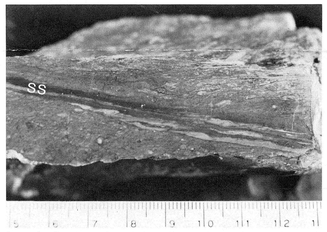

Figure 7. The slip surfaces (ss) are thin, continuous layers which consist of fine-grained recrystallized quartz. Sample AH1, XZ section. Sample viewed looking south. Centimeter scale.

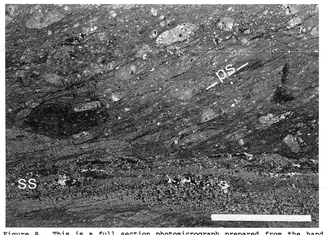

Figure 8. This is a full section photomicrograph prepared from the hand sample shown in Fig. 7. Some porphyroclasts of dolomite consist of recemented grain fragments, the occurrence of which is evidence for multiple generations of cataclasis. Pressure solution selvedges (pse) overprint the cataclastic fabric. The selvedges truncate the margins of the porphyroclasts creating an apparent elongation. The pressure solution selvedges are rotated into the younger slip surfaces (ss). This rotation can be used to deduce an east-over-west sense of displacement along the fault. Sample viewed looking south. Quartz within the slip surfaces is recrystallized to very fine grains which display a strong crystallographic preferred orientation. Sample AH1, XZ section. Crossed nicols. Bar scale is 5 millimeters.

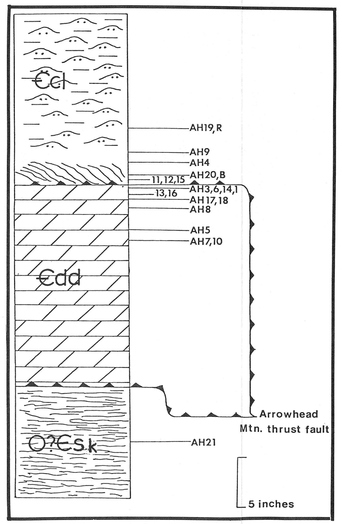

Figure 4. The column depicts the structural-stratigraphic relations at the sample locality of the Arrowhead Mountain thrust fault. The column is constructed as if the viewer is looking north. The Lower Member of the Cambrian Cheshire Quartzite (Ccl) is emplaced above the Ordovician (?) Cambrian Skeels Corners Slate (O?Csk). Slivers of Lower Cambrian Dunham Dolomite (Cdd) decorate the fault zone. The location of oriented samples is shown on the right side. Two thin sections were prepared from each sample. Both sections are cut perpendicular to the foliation; one section is parallel to the lineation (corresponding to an XZ section within a structural framework) and the other is perpendicular to the lineation.

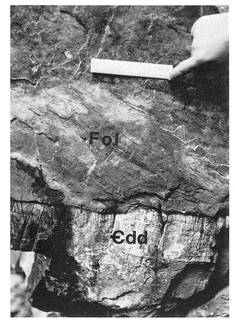

Figure 5. The upper thrust contact (T) between the quartzite (Fol) and the dolostone (Cdd) is the dominant slip surface because it is continuous within the fault zone. It is a sharp, planar interface. The quartzite (Fol) directly above the dolostone is highly foliated and densely impregnated with quartz veins whereas the quartzite above the fuler has argillaceous laminations and is more massive. The foliation in the lower part of the quartzite (Fol) is bent into near parallelism with the slip surface in the dolostone (Cdd) indicating east-over-west displacement. A thin transitional unit (T) occurs along the contact between the foliated quartzite (Fol) and the underlying dolostone. The view is to the north.

Figure 9. Full section photomicrograph of the tectonized transitional unit. This fabric group is characterized by a strongly developed foliation. Multiple generations of quartz veins, most of which are recrystallized to fine-grained aggregates, impregnate the rock. The tight folds are due to dissolution associated with the formation of pressure solution selvedges. Selvedge and vein formation occurred synchronously because they cross cut each other. Detrital grains and grain clusters may be slightly modified by recrystallization. Sample AH11, XZ section. Crossed nicols. Bar scale is 5 millimeters.

Description	Unit	Origin	Deformation Mechanism
angular fragments, poorly sorted, matrix	Cdd	microcracking, frictional sliding	cataclastic flow
deformation twins	Cdd	stress induced	low T plasticity
shear fractured porphyroclasts	Cdd	fracturing	cataclastic flow
stylolitic surfaces	Cdd	dissolution, concentration of insoluble residue	pressure solution
solution selvedges	Cdd, Ccl, TT		
slip surfaces of ultra-fine grained quartz	Cdd	migration of quartz-rich fluid along Y fractures	1. fracturing & fluid entry 2. recrystallization (dislocation creep)
quartz + dolomite veins (recrystallized)	Cdd, Ccl, TT	infilled fractures	pressure solution & hydraulic fracturing dislocation creep
elongate dolomite porphyroclasts	Cdd	dissolution	pressure solution
fibrous pressure shadows	Ccl		pressure solution
sericite beards	Ccl		pressure solution
rotated pressure solution selvedges	Cdd		
ghost porphyroclasts	Cdd	recementation by solution activity	pressure solution
buckle folded veins, offset veins	Ccl, TT	dissolution	pressure solution

Figure 10. Summary of microstructures observed in the dolomite (Cdd), quartzite (Ccl) and tectonized transitional unit (TT). The deformation mechanisms that were operative in each rock type are described.

Deformation Mechanism	Process	Deformation Product Microstructures	Inferred Dynamo-mechanical Model
Cataclastic Flow	Grain size reduction by macro- and micro-fracturing	Non-foliated cataclasites Microbreccias	Thinning of dolomite, attenuation of lower fold limb. Initial displacement occurs, energy is absorbed in the production of cataclasites. Stable sliding.
Solution Activity	Induration		Rock becomes stress supporting.
Renewed cataclasis		Ghost porphyroclasts	
Fracturing	Sliding occurs on discrete surface at dolomite-quartzite contact. Asperities are sheared off.	Dolomite lenses, formation of tectonized transitional unit.	Deformation becomes heterogeneous and localized along fractures. Stick slip motion.
Cyclic Pressure Solution and Hydraulic Fracturing	Pressure solution generates fluid. Periods of high fluid pressure coincide with hydraulic fracturing. Increased permeability causes influx of fluids and dissipation of high pressures. Extensive fluid migration occurs in the fault zone.	Dissolution of grains Stylolite formation Vein formation (several generations) Buckling of veins by dissolution.	
(Shear) Fracturing	Formation of slip surfaces which are y fractures. They are distant zones which quartz rich fluids enter.		
Localized Dislocation Creep	Recrystallization of slip surfaces.	Rotation of stylolitic surfaces. Ultra-fine grain size reduction of quartz in slip surfaces.	Inhomogeneous behavior. Renewed movement occurs and strain is accommodated along slip surfaces. Localized high stress. ($\sigma_1 - \sigma_3$ = 0.7 to 1.3Kb)

Figure 11. Structural evolution of the Arrowhead Mountain fault zone based on fabrics and microstructures. The sequence of events is shown from oldest (top) to most recent (bottom).

Studies in Vermont Geology No. 3, 1986 - Strehle and Stanley

Vermont Geological Survey, Charles A. Ratte, State Geologist

The Hinesburg Thrust Fault at Hinesburg

Plate 2

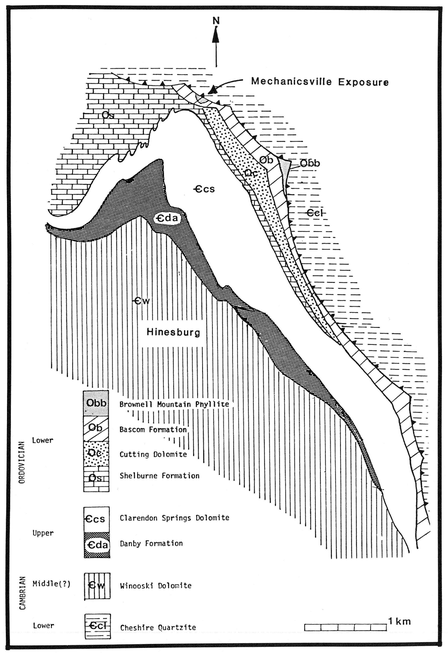

Figure 12. Geologic map of the Hinesburg thrust fault in the Mechanicsville area by Gillespie (1975). The Lower Member of the Lower Cambrian Cheshire Quartzite (Ccl) is emplaced above the Ordovician Bascom Formation (Ob) and Brownell Mountain Phyllite Member (Obb) which are locally disrupted. The Bascom Formation appears to rest unconformably on the Cutting, Shelburne, and Clarendon Springs Formation. The trace of the Hinesburg thrust fault is shown by a barbed line which has teeth on the upper plate.

Figure 13. The quartzite forms vertical south-facing cliffs above the less resistent gently sloping cumle-covered phyllite. S1 is parallel to the axial surface of tight to isoclinal F1 folds. The S1 foliation becomes mylonitic (Sm, mylonitic foliation) as the fault surface (bottom, out of field of view) is approached. Quartz veins are abundant. They formed in quartzite layers and older quartz veins. The quartz veins occur parallel to compositional layering (S0) and S1. 12-inch hammer indicates the scale.

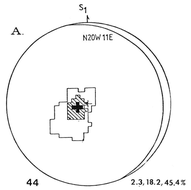

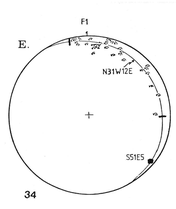

Figure 14. Lower hemisphere equal area projections of macroscopic fabric elements at the Mechanicsville locality. Projections A and B show the poles to 44 S1 surfaces and 18 S2 surfaces respectively. The surfaces corresponding to the maximum for each projection are represented by a great circle and labelled accordingly. Projection C shows 31 lithic lineations measured on S1. The orientation of the maximum trends S75E and plunges 10 degrees. Projection D shows the orientation of 5 mullions measured on the fault surface. The maximum trends S83E and plunges 18 degrees. Projection E shows the orientation of 34 F1 hinges measured throughout the outcrop and shown in figures 13 and 15. Circular arrows show the counterclockwise (east-over-west) sense of rotation of each fold. The F1 hinges define a great circle striking N31W and dipping 12° to the east which parallels S1 and the fault surface. The bisector of the separation arc, which is marked by tick marks, is shown by a dark square. It trends S51E and plunges at 5 degrees. The direction of motion on the Hinesburg thrust fault is given by the lineations in projections C and D which fall within the separation arc of diagram E. The sense of rotation of F1 folds indicates east-over-west motion along a direction slightly north of west.

ALL PICTURES ARE VIEWED TO THE NORTH

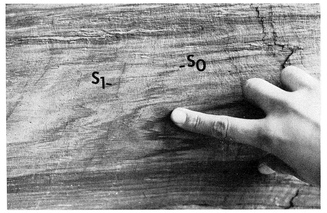

Figure 15. Compositional layering (S0) is partially to completely transposed by tight and isoclinal F1 folds. F1 folds occur throughout the argillaceous quartzite in figure 13 and are restricted to a 10 to 15 m zone above the thrust contact. F1 folds are formed by westward transport on the Hinesburg thrust fault. The compositional layering and associated foliation are related to the Hinesburg recumbent fold (Pl. 1, Fig. 1).

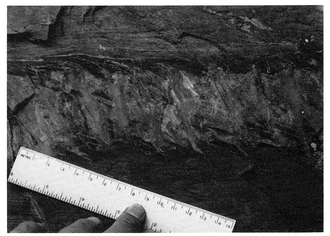

Figure 16. Dense quartz vein networks located above the hammer in Figure 13 are shown in more detail here. Although the quartz band occurs parallel to S1, the individual vein segments are at a high angle to S1. At least two generations of veins are present; the younger set is about 45 degrees to the foliation whereas the older set is at a lower angle. They are inferred to be infilled P fractures (e.g., Logan and others, 1979). The thin tails are rotated into parallelism with S1; the "Z" shape is consistent throughout the outcrop and indicates an east-over-west shear sense.

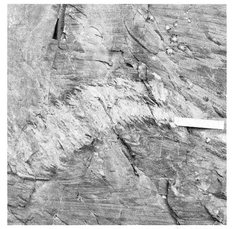

Figure 17. Thicker quartz veins are broadly folded. These veins are inferred to have developed during the early stages of S1 formation because they are deformed by F1 folds. The individual quartz segments within the broadly folded quartz vein are nearly parallel to the axial plane of the fold.

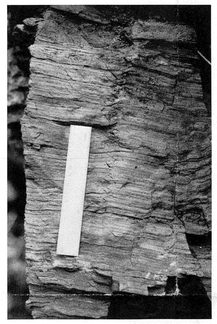

Figure 18. F2 folds produced broad undulations of the thrust surface. A weakly developed cleavage, S2, is sporadically developed and is coeval with F2. In contrast, Mesozoic deformation involved the formation of vertical fractures and kink bands located to the left of the 15 cm ruler.

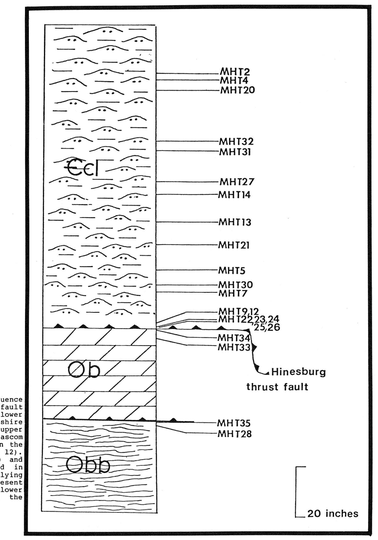

Figure 19. The rock sequence at the Hinesburg thrust fault at Mechanicsville. The lower member of the Cheshire Quartzite (Ccl) of the upper plate overlies the Bascom Formation (Ob) as shown on the geological map (Fig. 12). Slivers of dolostone (Ob) and phyllite (Obb) are found in contact with the overlying quartzite (Ccl) and represent material torn from the lower plate by movement along the fault.

	Feature	Location	Origin	Deformation Mechanism
Q U A R T Z	undulatory extinction	v , p	crystal lattice bending	dislocation glide
	deformation bands	v	polygonization	dislocation creep (recovery)
	marginal subgrains	v	polygonization	
	deformation lamellae, Boehm lamellae	p	requires electron microscopy	dislocation glide (?)
	subgrains	v	polygonization	dislocation creep (recovery)
	stretched crystals	v	recrystallization along areas of high strain (deformation bands)	dislocation creep
	ribbon texture grains	m	grain elongation and recrystallization	dislocation glide and dislocation creep
	ribbon grains (blades, ribbon porphyroclasts)	m	grain elongation	dislocation glide
FELDSPAR	deformation twins	p	stress induced (mechanical twinning)	twinning
	bent twins	p	crystal lattice bending	dislocation glide
	fractures	p	fracturing	fracturing
	undulatory extinction	p	crystal lattice bending	v-vein layer, p-porph-bearing sericite layers m-homogenous matrix highly deformed samples
OTHER	fractures (tourmaline, zircon)	p	fracturing	
	fibrous pressure snaows (pyrite)	p,m	pyrite pulls away from matrix creating zone of extension which is infilled	pressure solution

Figure 28. Summary of microstructures and deformation features observed in quartzite samples. The origin of these features and the operative deformation mechanism is also shown.

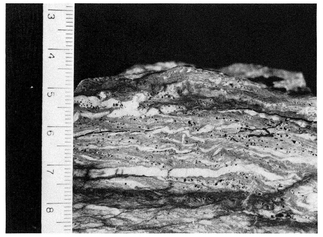

Figure 20. Pyrite (late S1 and pre-S1.5) within the quartzite increases in abundance as the fault surface is approached. Pits on the face of this sample (MHT9, XZ section) mark the former presence of pyrite porphyroblasts. Quartz veins (white bands), almost entirely recrystallized, occur parallel to S1. S1.5, a weak asymmetric spaced crenulation cleavage, is at a low angle (approximately 30 degrees) to S1 and is faintly visible within this sample. S1.5 is interpreted to be a shear band foliation which developed subsequent to Sm during the late, inhomogeneous stages of deformation. Centimeter and inch scale.

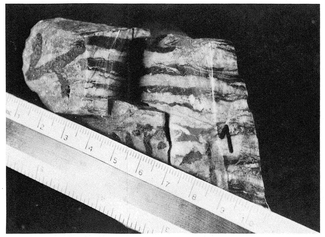

Figure 22. Sample MHT2 displays particularly well the common interlayering of quartz veins and phyllitic layers consisting mostly of sericite. The quartz veins occur parallel to S1. Centimeter and inch scale.

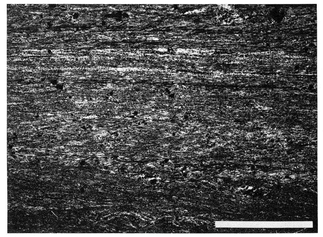

Figure 24. The S1 foliation becomes mylonitic as the thrust fault is approached. Sample MHT24 is an ultramylonite. Quartz grains have been deformed into thin, highly elongate ribbons. The mylonitic fault rocks are characterized by a strongly developed pervasive foliation in which grains and grain clusters are strongly elongated. This forms the lithic lineation shown in Figure 14c. XZ section. Crossed nicols. Bar scale at lower right is 5 millimeters.

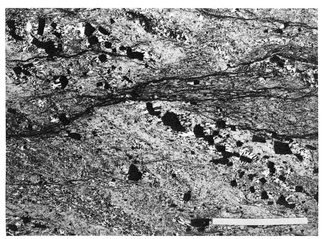

Figure 21 Full section photomicrograph of sample MHT9, XZ section (hand specimen is shown in figure 20). The sample consists of alternating layers of recrystallized quartz veins and sericite-chlorite layers. S1 is inclined to the right; S1.5 is horizontal. Pyrite porphyroblasts (post-Sm, pre-S1.5) have quartz-fiber pressure shadows. The fiber elongation direction is oriented at a low angle to S1.5. Crossed nicols. Bar scale is 5 millimeters.

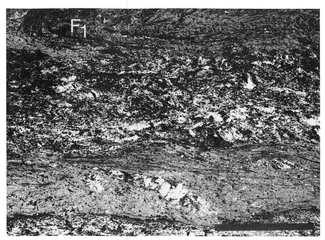

Figure 23. Full section photomicrograph of sample MHT2, XZ section. Quartz veins which are oriented parallel to S1 have undergone recrystallization. Thinner veins deformed into F1 folds originated as segregations parallel to compositional layering (S0). Relict F1 fold hinges are present in sericite layers. Crossed nicols. Bar scale at lower right is 5 millimeters.

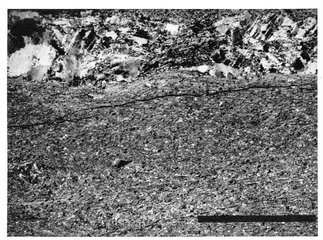

Figure 25. Further from the thrust fault, the quartz veins are not as extensively recrystallized. Porphyroclasts of detrital quartz and feldspar surrounded by the sericite matrix are undeformed. The quartz grains within the veins are polygonized into an array of subgrains. New grains preferentially nucleate at deformation band boundaries creating a segmentation of the porphyroclasts. Sample MHT20, XZ section. Crossed nicols. Bar scale at lower right is 5 millimeters.

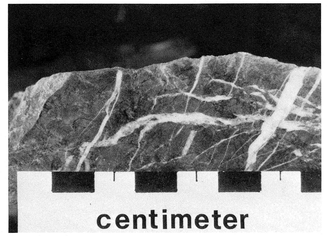

Figure 26. The dolomite of the Bascom Formation is densely impregnated with quartz and, in lesser amounts, carbonate and plagioclase, veins. The presence of these veins further substantiates the introduction of quartz-rich fluids into the fault zone. Sample MHT34.

Figure 27. Full section photomicrograph of sample MHT34, XZ section, crossed nicols. The Bascom Formation carbonate consists of uniformly fine-grained, anhedral, stylolitic dolomite. Several generations of quartz veins are present. They have undergone minor recrystallization and some exhibit a remnant fibrous habit. Bar scale at lower right is 5 millimeters.

Deformation Event	Folds	Nature of Foliation	Major Structural Event	Mesoscopically Visible Features	Microstructure	Deformation Mechanism
D_1	F_1 tight to isoclinal	S_1 axial planar	Nappe stage : Progressive formation of discrete sliding surface by attenuation of overturned limb. : Extensive quartz rich fluid migration along fault. :	Partial to complete transposition of bedding Tight to isoclinal minor folds Quartz veins (syn-S1-folded, late S1-parallel S1) Dominant surface along which rock breaks	Differentiated layering quartz-mica segregation Pyrite mineralization Pressure solution seams	Pressure Solution
Dm		Sm mylonitic parallel S1 (recognized by mylonitic fabric)	Translation of thrust-nappe structure : Locking :	Rotation and thinning of quartz digitations Dolomite becomes vein impregnated	Ribbon grains of quartz, microdigitations mylonitization Fracturing subpendicular to Sm, veins oblique to Sm. Pyrite mineralization Rare fibrous pressure shadows parallel Sm	Dislocation Creep Pressure Solution
D1.5		S1.5 nonpenetrative asymmetric spaced shear band foliation	Renewed movement of fault	Slight crenulation of Sm	Shear bands Fibrous pressure shadows Recrystallization of post-Sm veins	Pressure Solution, Dislocation Creep
D_2	F_2 open, rare	not observed	Folding of the thrust (Hinesburg Synclinorium)	Broad undulations of thrust surface		
D_3	Fractures, faults	S_3, rare kink folds	Normal faulting, brittle fracturing	Vertical fractures		

Figure 29. Chronology of structural events and related fabric and deformation mechanisms.

Studies in Vermont Geology No. 3, 1986 - Strehle and Stanley

Vermont Geological Survey, Charles A. Ratte, State Geologist

The Underhill Thrust Fault at South Lincoln

Plate 3

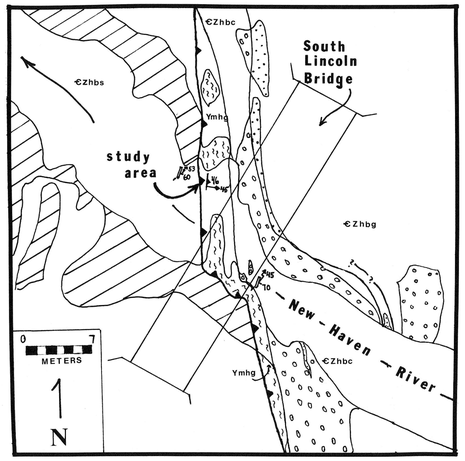

Figure 30. At the bridge at South Lincoln, the mylonitic gneiss of the Mt. Holly Complex (Ymhg) is in thrust contact with the Hoosac Formation (€Zhbs). A pervasive, platy mylonitic foliation (Sm) and penetrative mineral lineation dominates the gneiss (represented by symbols in gneiss sliver, Ymhg, and shown by the contoured data in Figure 33). The fault is deformed by younger folds (F2) represented by the symbols to the east and west of the sliver. In Jerusalem, the fault-related deformation along the Underhill thrust fault (Utf) is distributed over a much wider zone and numerous tectonic slivers are juxtaposed in the fault zone (fig. 45, Plate 4). Geology mapped by Tavers (1982) and modified by Stanley.

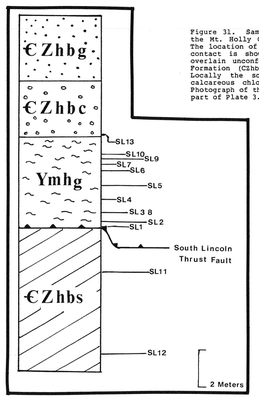

Figure 31. Samples were collected from the mylonitic gneiss of the Mt. Holly Complex (Ymhg) and the Hoosac Formation (€Zhbs). The location of sample collection sites with respect to the fault contact is shown to the right. The gneiss sliver, which is overlain unconformably by the basal conglomerate of the Hoosac Formation (€Zhbc), is emplaced from the east over the schist. Locally the schist can be divided into two units, a green calcareous chlorite schist and a darker grey biotite schist. Photograph of the outcrop is shown in figure 32 on the lower right part of Plate 3.

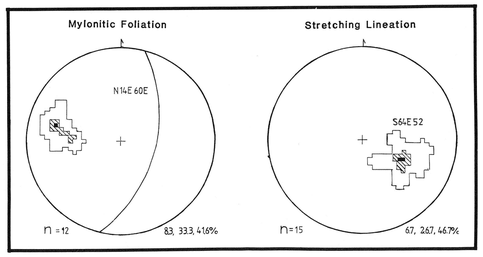

Figure 33. Lower hemisphere equal area projections of n poles to the mylonitic foliation and n stretching lineations. Tick marks north. Contours are given as the percentage of points per 1% area. The stretching lineation is defined by elongation of quartz and feldspar grains.

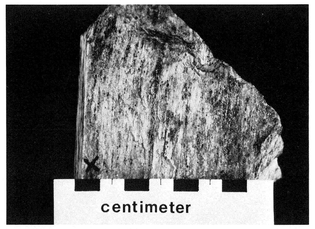

Figure 34. The mylonitic foliation displays a well developed mineral lineation. The lineation is formed by the elongation of quartz and feldspar grains. Sample SL4, Sm surface.

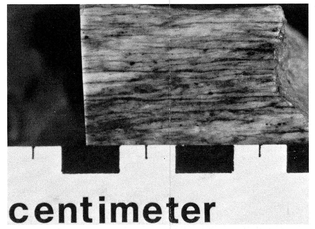

Figure 35. The mylonitic gneiss consists of quartz, plagioclase, muscovite and biotite with minor epidote and opaques. Samples display little variation in fabric but do vary compositionally in the amount of mica present. The foliation appears planar in sections (XZ) cut parallel to the lineation. Sample SL3, XZ section.

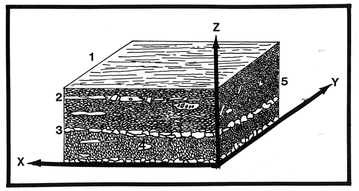

Figure 42. Schematic block diagram of microstructures observed in the mylonitic gneiss. 1: Well-developed pervasive stretching lineation defined by elongate quartz and feldspar grains on Sm (XY plane). 2: Slightly deformed biotite and muscovite occur both parallel and oblique to Sm. They are late-syn to post-Sm phases. 3: Quartz segregations occur parallel to Sm. They are late-Sm phases. 4: Plagioclase porphyroclasts are highly elongate, mildly saussuritized and display internal features resembling peristerite exsolution lamellae. 5: New grains of quartz and plagioclase appear less elongate in sections perpendicular to the lineation. Quartz bands are less regularly defined.

	Microstructure	Origin	Comments	Deformation Mechanism
QUARTZ	Porphyroclast elongation, deformation bands		scalloped and embayed boundaries, grains are located in the matrix	Dislocation glide and dislocation creep (recovery)
	Imbricated elongate new grains	Dynamic recrystalli-zation	Strong preferred orientation	Dislocation creep
	New grain aggregates	Dynamic recrystalli-zation	Grains are commonly undulose, majority are elongate (in XZ sections)	Dislocation creep
	Elongate domains	Late stage quartz segregations which have undergone subse-quent deformation	Similar to ribbon micro-structure of Bouchez & Pecher (1981) and Bouchez (1982)	Dislocation creep (recovery)
FELDSPAR	Undulatory Extinction porphs			
	Mechanical twins(?)	Deformation twinning		Low T plasticity
	New grains of plagioclase		Recrystallization occurs at T 450°, grains may have single and poly-synthetic twins	Dislocation Creep
	Bent cleavage and twins	Crystal lattice bending		
	Marginal new grains	Recrystallization at grain margins		Dislocation Creep
	Stuffed crystals			
	"Tweed" microstructure	Exsolution(?)	Temperatures after growth were high enough to allow reordering	Diffusion or Dislocation Creep
MICA	Strong preferred orientation	Growth late syn to post S_m	Crystals show little evidence of deformation	Diffusion
	Fine grained mica oblique to S_m	Recrystallization of older grains		
	Undulatory extinction			
	Coarse grained subhedral mica oblique to S_m	Growth late to post S_m		Diffusion

Figure 43. Summary of microstructures and deformation features observed in quartz, plagioclase feldspar and mica in the mylonitic gneiss. The associated deformation mechanism is also given.

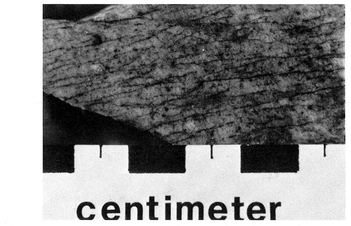

Figure 36. In sections cut perpendicular to the lineation, the foliation has an anastomosing geometry. The mica weaves around the equant-end sections of elongate grains. Sample SL3, YZ section.

Figure 37. Quartz and plagioclase are almost entirely recrystallized. Quartz, which is segregated into layers parallel to the mylonitic foliation (Sm), exhibits evidence of recovery (deformation bands). These layers are interpreted to have segregated during or after the formation of Sm. Subsequent deformation resulted in the development of deformation bands. Structural analysis was conducted on this sample (SL3) to determine whether an asymmetry, which could be used to determine the sense of shear, was preserved in the crystallographic fabric (Fig. 38). Crossed nicols. Bar scale is 5 millimeters.

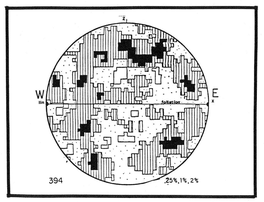

Figure 38. Lower hemisphere equal area projection of 394 quartz C-axes from sample SL3. The data area projected onto the XZ plane which parallels the lineation and is perpendicular to the foliation (parallel to the N-E line on the diagram). Contours are given as the percentage of points per 1% area. Measurements were collected from two mutual perpendicular sections (XZ and YZ). The sample population consisted almost entirely of quartz grains in the layers parallel to the foliation. The pattern does not display a clear asymmetry. The diffuseness is attributed to the effects of recovery processes (i.e. development of deformation bands in quartz) which would not be expected to produce a preferred orientation of C-axes. Furthermore, it is unlikely that the quartz was originally oriented because they were segregated during the late- to post-Sm phase of deformation.

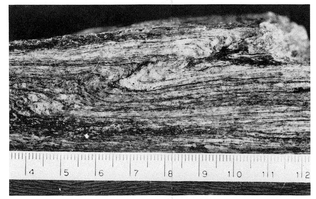

Figure 39. Tight to isoclinal folds deform the mylonitic foliation. These folds are best developed in mica-rich samples. In this sample (SL9), the fold slips out along the mica-rich layers. These folds (incipient sheath folds?) are interpreted to result from post-Sm displacement along the fault. Sample SL9. YZ section. Centimeter scale.

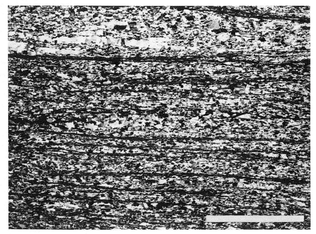

Figure 40. Sample SL9 is very micaceous. It also contains quartz layers. U-stage analysis of the quartz C axes within this sample did not reveal an asymmetry.

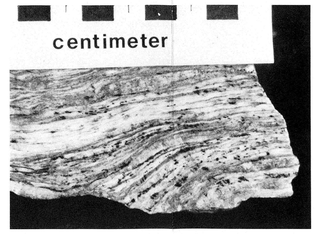

Figure 41. Crenulations are sporadically developed in the mylonitic gneiss. They are correlated with F2 folds which deform the thrust fault and are responsible for the open folds in the Hoosac Formation. These folds are represented by structural symbols to the east and west of the Mt. Holly sliver (Ymhg) in Figure 30. Cross biotites post-date the crenulation cleavage. They indicate that moderate temperatures associated with the second metamorphic event (M2) persisted after deformation.

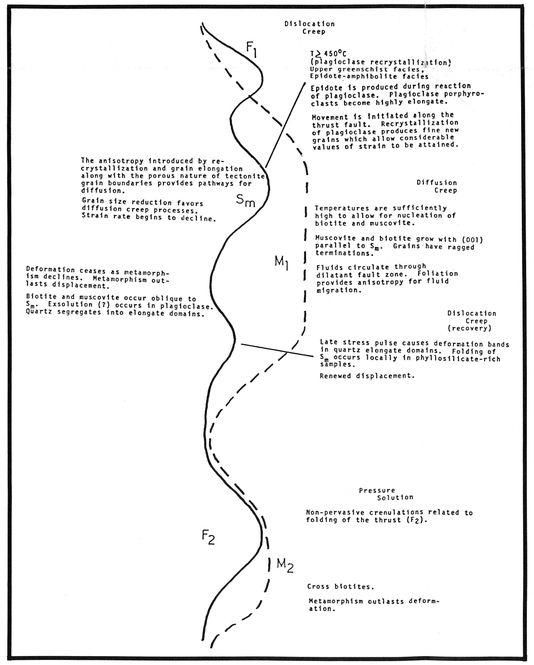

Figure 44. Synoptic evolutionary diagram that relates deformation and metamorphism inferred from the data observed in outcrop and thin section from the thrust zone at South Lincoln.

Figure 32. The thrust fault along the east bank of the New Haven River at South Lincoln. The darker rocks to the left are chlorite, biotite schist of the Hoosac Formation (€Zhbs). The lighter colored rocks to the right are the mylonitic gneiss of the Mt. Holly Complex (Ymhg). The contact between the two units is the thrust fault. The basal conglomerate of the Hoosac Formation (€Zhbc) is exposed to the right of the photograph below the South Lincoln bridge. Younger folds deform the dominant foliation and the thrust contact. View looking to the northeast.

Studies in Vermont Geology No. 3, 1986 - Strehle and Stanley

Vermont Geological Survey, Charles A. Ratte, State Geologist

The Underhill Thrust Fault at Jerusalem

Plate 4

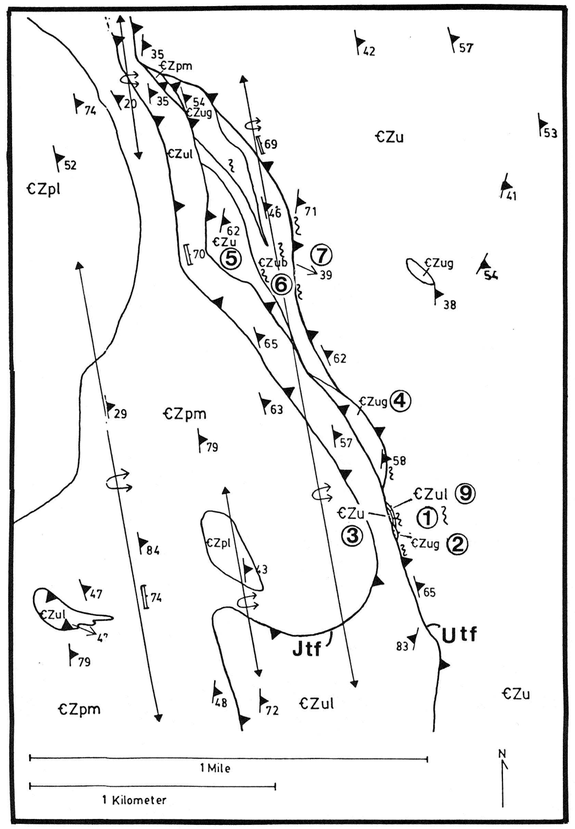

Figure 45. Geologic map of the Underhill thrust fault (Utf) at Jerusalem as mapped by DiPietro (1983). Sample localities are shown by number. The Underhill thrust fault overlies the Jerusalem thrust fault (Jtf) and contains slivers of greenstone (CZug), biotite metagraywacke (CZub), and quartz-sericite schist (CZu).

Figure 46. Mylonitic quartzites occur along the Underhill thrust fault in Jerusalem. The mylonites are strongly foliated and display a well-developed down dip lineation (parallel to 6-inch ruler). These mylonites are interpreted to have originated as schistosity parallel quartz veins which segregated in the early stages of deformation and were subsequently recrystallized during shearing.

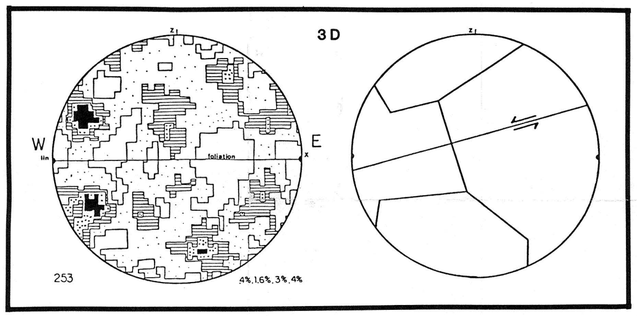

Figure 48. Universal stage analysis of quartz c-axes revealed a distinct asymmetry in the crystallographic fabric (a). Both the distribution intensity and the fabric skeleton (b) indicate an east-over-west shear sense. C-axes are shown as lower hemisphere equal area projections onto the XZ plane. The lineation and foliation are shown on the contoured projection. 253 c-axes, contours are given as the percentage of points per 1% area.

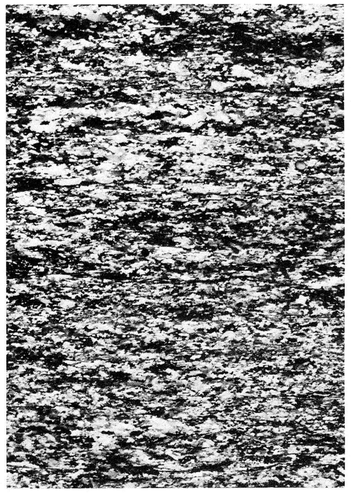

Figure 47. Sample 3D is a mylonite from a sheared quartz vein. Quartz is entirely recrystallized to fine-grained aggregates of new grains that exhibit a strong crystallographic preferred orientation. Crossed nicols. Bar scale is 5 millimeters.

Figure 49. Microstructures were utilized to determine the shear sense. Polyphase rocks such as the metabasites, which consist of coarse-grained biotite, hornblende, actinolite, muscovite and chlorite in addition to finer-grained sphene, quartz, plagioclase, calcite and iron oxides, are well-suited to microstructural shear sense analysis. The deformed biotite indicates an east-over-west shear sense when transformed into a geographic coordinate system. Sample 2D. Crossed nicols. Bar scale is 5 millimeters.

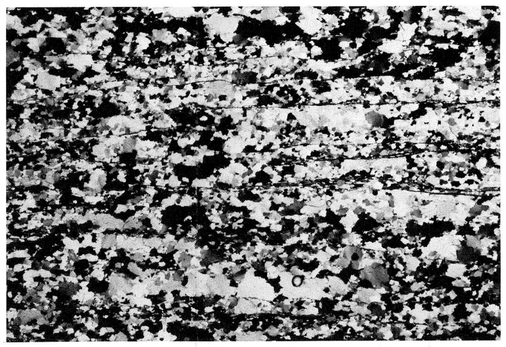

Figure 50. Some of the quartz mylonites within the Underhill thrust fault zone exhibit fabrics which result from grain growth coarsening subsequent to deformation. Grains are much coarser and have blotchy shapes. These grains commonly enclose fine grains of sericite. Sample 5A, XZ section. Crossed nicols. Bar scale is 5 millimeters.

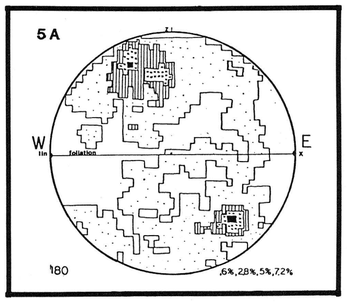

Figure 51. Quartz c-axis analysis of fabrics which exhibit grain growth coarsening also reveal an east-over-west asymmetry. The pattern, however, does not resemble typical distributions such as the crossed girdle obtained for sample 3D. Lower hemisphere equal area projection of 180 c-axes onto the XZ plane. Contours are shown as the percentage of points per 1% area (lower right corner).

Studies in Vermont Geology No. 3, 1986 - Strehle and Stanley

Vermont Geological Survey, Charles A. Ratte, State Geologist